Critical exponents and equation of state of the three-dimensional Heisenberg universality class

Massimo Campostrini,[1,*] Martin Hasenbusch,[2,†] Andrea Pelissetto,[3,‡] Paolo Rossi,[1,§] and Ettore Vicari[1,‖]
[1]*Dipartimento di Fisica dell'Università di Pisa and I.N.F.N., I-56126 Pisa, Italy*
[2]*NIC/DESY Zeuthen, Platanenallee 6, D-15738 Zeuthen, Germany*
[3]*Dipartimento di Fisica dell'Università di Roma I and I.N.F.N., I-00185 Roma, Italy*
(Received 16 October 2001; published 2 April 2002)

We improve the theoretical estimates of the critical exponents for the three-dimensional Heisenberg universality class. We find $\gamma=1.3960(9)$, $\nu=0.7112(5)$, $\eta=0.0375(5)$, $\alpha=-0.1336(15)$, $\beta=0.3689(3)$, and $\delta=4.783(3)$. We consider an improved lattice ϕ^4 Hamiltonian with suppressed leading scaling corrections. Our results are obtained by combining Monte Carlo simulations based on finite-size scaling methods and high-temperature expansions. The critical exponents are computed from high-temperature expansions specialized to the ϕ^4 improved model. By the same technique we determine the coefficients of the small-magnetization expansion of the equation of state. This expansion is extended analytically by means of approximate parametric representations, obtaining the equation of state in the whole critical region. We also determine a number of universal amplitude ratios.

DOI: 10.1103/PhysRevB.65.144520 PACS number(s): 75.10.Hk, 05.70.Jk, 11.15.Me

I. INTRODUCTION AND SUMMARY

According to the universality hypothesis, some features of continuous phase transitions–for instance, critical exponents and scaling functions—do not depend on the microscopic details of the systems, but only on a few global properties, such as the space dimensionality, the range of interaction, and the symmetry of the order parameter. These features define a universality class. In this paper, we consider the three-dimensional Heisenberg universality class, which is characterized by a three-component order parameter, $O(3)$ symmetry, and short-range interactions.

The Heisenberg universality class describes[1] the critical behavior of isotropic magnets, for instance the Curie transition in isotropic ferromagnets such as Ni and EuO, and of antiferromagnets such as $RbMnF_3$ at the Néel transition point. In Table I we report some recent experimental results. It is not a complete review of published results, but is useful to give an overview of the experimental state of the art. In the table we also included results for the well-studied doped manganese perovskites $La_{1-x}A_xMnO_3$, although the nature of the ferromagnetic transition in these compounds is still unclear.[15] The Heisenberg universality class also describes isotropic magnets with quenched disorder. Indeed, since $\alpha<0$, the Harris criterion states that disorder is an irrelevant perturbation. The only effect is to introduce a correction-to-scaling term $|t|^{\Delta_{\rm dis}}$ with $\Delta_{\rm dis}=-\alpha$. The experimental results confirm the theoretical analysis,[16] as can be seen from Table II (older experimental results with a critical discussion were reported in Ref. 24). The prediction for $\Delta_{\rm dis}$ was checked in perturbative field theory[25] and experimentally.[26,18,19]

Beside the exponents γ, β, and δ, there are also a few estimates of the specific-heat exponent α, in most of the cases obtained from resistivity measurements: $\alpha\approx-0.10$ in Fe and Ni,[27] $\alpha=-0.12(2)$ in EuO,[28] $\alpha=-0.11(1)$ in $Fe_xNi_{80-x}B_{19}Si$,[17] and $\alpha=-0.11(1)$ in $RbMnF_3$.[29]

The aim of this paper is to substantially improve the precision of the theoretical estimates of the critical exponents. For this purpose, we consider an improved lattice Hamiltonian that is characterized by the fact that the leading correction to scaling is (approximately) absent in the expansion of any observable near the critical point. Moreover, we combine Monte Carlo (MC) simulations and analyses of high-temperature (HT) series. We exploit the effectiveness of MC simulations and finite-size scaling (FSS) techniques to determine the critical temperature and the parameters of the improved Hamiltonians,[30–37] and the effectiveness of HT methods to determine the critical exponents for improved models, especially when a precise estimate of the critical point is available. This approach was already applied to the three-dimensional Ising[38] and XY (Refs. 39 and 36) universality classes, achieving a substantial improvement of the estimates of the universal quantities that describe the critical behavior, such as the critical exponents and the scaling equation of state.

We consider a simple cubic lattice and the nearest-neighbor ϕ^4 lattice Hamiltonian

$$\mathcal{H}_{\phi^4}=-\beta\sum_{\langle xy\rangle}\vec{\phi}_x\cdot\vec{\phi}_y+\sum_x\left[\vec{\phi}_x^{\,2}+\lambda(\vec{\phi}_x^{\,2}-1)^2\right], \qquad (1)$$

where $\vec{\phi}_x$ is a three-component field. As shown in Ref. 37, Hamiltonian (1) is improved for $\lambda=\lambda^*\approx4.4(7)$. Here we extend the simulations of Ref. 37, obtaining a more accurate estimate of λ^*, $\lambda^*=4.6(4)$, and precise estimates of the critical β_c for several values of λ. The analysis of the MC FSS results obtained for the improved ϕ^4 lattice Hamiltonian already provides precise estimates of the critical exponents. As shown in Refs. 38, 39, and 36, an additional increase in precision can be obtained by combining improved Hamiltonians and HT methods. For this purpose, by using the linked-cluster expansion technique, we computed HT expansions of several quantities and analyzed them using the MC results for λ^* and β_c. The final results significantly improve those obtained from the MC simulation. Moreover, they substan-

TABLE I. Recent experimental estimates of the critical exponents for Heisenberg systems.

	Material	γ	β	δ
Ref. 2 (1980)	Ni		0.354(14)	
Ref. 3 (1981)	Fe		0.367(5)	
Ref. 4 (1995)	Ni	1.345(10)	0.395(10)	4.35(6)
Ref. 5 (1995)	Gd_2BrC	1.392(8)	0.365(5)	4.80(25)
Ref. 5 (1995)	Gd_2IC	1.370(8)	0.375(8)	4.68(25)
Ref. 6 (1999)	$Tl_2Mn_2O_7$	1.31(5)	0.44(6)	4.65(15)
Ref. 7 (2000)	$La_{0.82}Ca_{0.18}MnO_3$		0.383(9)	
Ref. 8 (2000)	$La_{0.95}Ca_{0.05}MnO_3$	1.39(5)	0.36(7)	4.75(15)
Ref. 9 (2000)	Gd(0001)		0.376(15)	
Ref. 10 (2000)	Gd_2CuO_4	1.32(2)	0.34(1)	
Ref. 11 (2000)	$C_{80}Pd_{20}$ (liq)	1.42(5)		
Ref. 11 (2000)	$C_{80}Pd_{20}$ (sol)	1.40(8)		
Ref. 12 (2001)	GdS		0.38(2)	
Ref. 13 (2001)	CrO_2	1.43(1)	0.371(5)	
Ref. 14 (2001)	$La_{0.8}Ca_{0.2}MnO_3$	1.45	0.36	

tially improve those obtained using longer (21 orders) series for the standard Heisenberg model.[40]

In Table III we report our results for the critical exponents. We give the estimates obtained from the analysis of the MC data alone and those obtained by combining MC and HT techniques—they are denoted by MC+IHT, where the ''I'' refers to the fact that we are considering an improved model. The exponent α can be derived using the hyperscaling relation $\alpha=2-3\nu$, obtaining $\alpha=-0.1336(15)$. We would like to stress that the good agreement between the MC and HT estimates is not trivial, since the critical exponents are determined from different quantities and limits. Indeed, the MC estimates are obtained from the analysis of the finite-size behavior for the size $L\to\infty$ at the critical point $\beta=\beta_c$, while the HT results are derived from the singular behavior of infinite-volume quantities as $\beta\to\beta_c$.

In Table III we compare our results with the most precise theoretical estimates obtained in recent years. A more complete list of results can be found in Ref. 56. The results we quote have been obtained by Monte Carlo simulations, from the analysis of the HT series for the standard Heisenberg model, or by field-theory methods (FT). The MC results were obtained by applying FSS techniques to different Hamiltonians. References 42–44 studied the standard $O(3)$-vector Heisenberg model, Ref. 37 the improved ϕ^4 model, and Ref. 41 an isotropic ferromagnet with double-exchange interactions.[57] The HT results of Ref. 40 were obtained analyzing the 21st-order HT expansions for the standard $O(3)$-vector model on the simple cubic (sc) and on the body-centered cubic (bcc) lattice. The FT results of Refs. 46–51 were derived by analyzing perturbative expansions in different frameworks: fixed-dimension expansion (sixth- and

TABLE II. Recent experimental estimates of the critical exponents for Heisenberg systems with quenched disorder.

	Material	γ	β	δ
Ref. 17 (1994)	$Fe_{10}Ni_{70}Bi_{19}Si$	1.387(12)	0.378(15)	4.50(5)
Ref. 17 (1994)	$Fe_{13}Ni_{67}Bi_{19}Si$	1.386(12)	0.367(15)	4.50(5)
Ref. 17 (1994)	$Fe_{16}Ni_{64}Bi_{19}Si$	1.386(14)	0.360(15)	4.86(4)
Refs. 18 and 19 (1995)	$Fe_{20}Ni_{60}P_{14}B_6$	1.386(10)	0.367(10)	4.77(5)
Refs. 18 and 19 (1995)	$Fe_{40}Ni_{40}P_{14}B_6$	1.385(10)	0.364(5)	4.79(5)
Ref. 20 (1997)	$Fe_{91}Zr_9$	1.383(4)	0.366(4)	4.75(5)
Ref. 20 (1997)	$Fe_{89}CoZr_{10}$	1.385(5)	0.368(6)	4.80(4)
Ref. 20 (1997)	$Fe_{88}Co_2Zr_{10}$	1.389(6)	0.363(5)	4.81(5)
Ref. 20 (1997)	$Fe_{84}Co_6Zr_{10}$	1.386(6)	0.370(5)	4.84(5)
Ref. 21 (1999)	$Fe_{1.85}Mn_{1.15}Si$	1.543(20)	0.408(60)	4.74(7)
Ref. 21 (1999)	$Fe_{1.50}Mn_{1.50}Si$	1.274(60)	0.383(10)	4.45(19)
Ref. 22 (2000)	$Fe_{86}Mn_4Zr_{10}$	1.381	0.361	
Ref. 22 (2000)	$Fe_{82}Mn_8Zr_{10}$	1.367	0.363	
Ref. 23 (2001)	$Fe_{84}Mn_6Zr_{10}$	1.37(3)	0.359	4.81(4)
Ref. 23 (2001)	$Fe_{74}Mn_{16}Zr_{10}$	1.39(5)	0.361	4.86(3)

TABLE III. Estimates of the critical exponents. See the text for the explanation of the symbols in the second column. We indicate with an asterisk (*) the estimates that were obtained using the relations $\gamma=(2-\eta)\nu$, $2\beta=\nu(1+\eta)$, and $\delta(1+\eta)=5-\eta$.

Ref.	Method	γ	ν	η	β	δ
this work	MC+IHT	1.3960(9)	0.7112(5)	0.0375(5)	0.3689(3)*	4.783(3)*
this work	MC	1.3957(22)*	0.7113(11)	0.0378(6)	0.3691(6)*	4.781(3)*
37 (2000)	MC	1.393(4)*	0.710(2)	0.0380(10)	0.3685(11)*	4.780(6)*
41 (2000)	MC	1.3909(30)	0.6949(38)		0.3535(30)	
42 (1996)	MC	1.396(3)*	0.7128(14)	0.0413(16)	0.3711(9)*	4.762(9)*
43 (1993)	MC	1.389(14)*	0.704(6)	0.027(2)	0.362(3)*	4.842(11)*
44 (1991)	MC	1.390(23)*	0.706(9)	0.031(7)	0.364(5)*	4.82(4)*
40 (1997)	HT sc	1.406(3)	0.716(2)	0.036(7)*	0.3710(13)*	4.79(4)*
40 (1997)	HT bcc	1.402(3)	0.714(2)	0.036(7)*	0.3700(13)*	4.79(4)*
45 (1993)	HT	1.40(1)	0.712(10)	0.03(3)*	0.368(6)*	
46 (2001)	FT $d=3$ exp	1.3882(10)	0.7062(7)	0.0350(8)	0.3655(5)*	4.797(5)*
47 (1998)	FT $d=3$ exp	1.3895(50)	0.7073(35)	0.0355(25)	0.3662(25)	4.794(14)
48 (1991)	FT $d=3$ exp	1.3926(13)[39]	0.7096(8)[22]	0.0374(4)		
49 (1977)	FT $d=3$ exp	1.386(4)	0.705(3)	0.033(4)	0.3645(25)	4.808(22)
47 (1998)	FT ϵ-exp	1.382(9)	0.7045(55)	0.0375(45)	0.3655(35)	4.783(25)
50 (1998)	FT ϵ-exp	1.39*	0.708	0.037	0.367*	4.786*
51 (2000)	FT $(d-2)$-exp		0.695(10)			
52 (1984)	SFM	1.40(3)	0.715(20)	0.044(7)	0.373(11)	4.75(4)*
53 (2001)	CRG		0.74	0.038	0.37	4.78
54 (2001)	CRG	1.374	0.704	0.049	0.369	4.720
55 (1996)	CRG	1.465	0.747	0.038	0.388	4.78

seventh-order series; see Refs. 58 and 48), ϵ expansion [to $O(\epsilon^5)$, see Refs. 59 and 60], and $(d-2)$ expansion (to $O[(d-2)^4]$; see Refs. 61–63). We quote two errors for the results of Ref. 48: the first one (in parentheses) is the resummation error, and the second one (in brackets) takes into account the uncertainty of the fixed-point value g^* of the coupling, which was estimated to be approximately 1% in Ref. 48. To estimate the second error we use the results of Ref. 47, where the dependence of the exponents on g^* is given. The results of Ref. 52 were obtained by using the so-called scaling-field method (SFM). References 53–55 and 64 presented results obtained by approximately solving continuous renormalization-group (CRG) equations for the average action, which is approximated to lowest and first order of the derivative expansion. We also mention the HT results of Ref. 65: they performed a direct determination of the exponent α obtaining $\alpha=-0.11(2)$ and $-0.13(2)$ on the sc and bcc lattices. Reference 66 computed the critical exponents for a Heisenberg fluid by a canonical-ensemble simulation. Depending on the analysis method, they found $1/\nu=1.40(1)$, $1.31(1)$, $\beta/\nu=0.54(2)$, $0.52(1)$, and $\gamma/\nu=1.90(3)$, $1.87(3)$. Overall, all estimates are in substantial agreement with our MC+IHT results. We only note the apparent discrepancies with the MC estimates of η of Refs. 42 and 43, and with the FT results of Ref. 46. However, the reliability of the error bars reported in Ref. 46 is unclear: indeed, Ref. 47 analyzed the same perturbative series, and reported much more cautious error estimates.

We also present a detailed study of the equation of state. We first consider its expansion in terms of the magnetization in the HT phase. The coefficients of this expansion are directly related to the zero-momentum n-point renormalized couplings, which are determined by analyzing their HT expansion. These results are used to construct parametric representations of the critical equation of state which are valid in the whole critical region, satisfy the correct analytic properties (Griffiths' analyticity), and take into account the Goldstone singularities at the coexistence curve. From our approximate representations of the equation of state we derive estimates of several universal amplitude ratios. Moreover, we present several results and different forms of the equation of state that can be compared directly with experiments. In particular, we can compare with the experimental results of Refs. 17, 20, and 6, finding good agreement.

The paper is organized as follows. In Sec. II we present our MC results. In Sec. III we present our results for the critical exponents obtained from the analysis of the HT series for the improved Hamiltonian [Eq. (1)]. The equation of state is discussed in Sec. IV. We determine the small-magnetization expansion coefficients in Sec. IV A, give an approximate parametric representation of the equation of state in Secs. IV B and IV C, compute several amplitude ratios in Sec. IV D, and compare the theoretical results with experimental data in Sec. IV E. Details are reported in the Appendixes. In Appendix A we present an analysis of the MC results and in Appendix B an analysis of the HT series. The expressions of several amplitude ratios in terms of the parametric representations are reported in Appendix C.

II. MONTE CARLO SIMULATIONS

The present MC simulations extend those of Ref. 37. Here we have considerably enlarged the statistics and added larger

TABLE IV. Final results for β_c and R^* from fits with ansatz (2). In parentheses we give the statistical error, and in brackets the error due to the corrections to scaling.

R	Z_a/Z_p	$\xi_{2\mathrm{nd}}/L$	U_4	U_6
R^*	0.1944(1)[4]	0.5644(1)[2]	1.1394(1)[2]	1.4202(2)[10]
β_c	0.6862390(10)[12]	0.6862386(11)[6]	0.6862365(17)[12]	0.6862369(17)[19]

lattice sizes. Moreover, we have considered an additional quantity in order to improve the control over systematic errors. This way, we can increase the accuracy of λ^* and give precise estimates of the critical β_c for three values of λ in a neighborhood of λ^*. For a detailed discussion of our methods, see Ref. 36. Details are reported in Appendix A.

We simulated the $O(3)$-symmetric ϕ^4 model (1) at $\lambda = 4.0$, 4.5, and 5.0 on a simple cubic lattice with linear extension L in all directions. We measured the Binder parameter U_4, its sixth-order generalization U_6, the second-moment correlation length $\xi_{2\mathrm{nd}}$, and the ratio Z_a/Z_p, where Z_a is the partition function with antiperiodic boundary conditions in one of the three directions and Z_p the corresponding one with periodic boundary conditions in all directions. The number of iterations for each lattice size and value of λ was approximately 10^7 for $L=6$, 7, 8, 9, 10, 11, 12, 14, 16, 18, 20, and 22, approximately 10^6 for $L=24$, 28, 32, 36, 40, and 48, and $(1-4)\times 10^5$ for $L=56$, 64, 80, and 96. With respect to Ref. 37, we have added lattice sizes for all three values of λ and considerably increased the statistics. In total, the whole study took about four years on a single 450-MHz Pentium III CPU.

In the first step of the analysis, we compute β_c and the fixed-point value of the dimensionless ratios R^* for $\lambda=4.5$, using the standard cumulant crossing method of Binder. In particular, we fit our data with the ansatz

$$R^* = R(L,\beta_c), \tag{2}$$

where R^* and β_c are free parameters. Our results are reported in Table IV. Note that the four results for β_c are consistent within error bars. The statistical error of β_c obtained from Z_a/Z_p and $\xi_{2\mathrm{nd}}/L$ is considerably smaller than that from U_4 and U_6. As our final estimate we take $\beta_c = 0.6862385(20)$, which is consistent with all four results.

In addition, we determine β_c for $\lambda=4.0$ and 5.0. For this purpose, we use ansatz (2), fixing $L=96$ and taking the values of R^* from Table IV. Our results are summarized in Table V. For both values of λ, the results obtained from the four different choices of R^* are consistent within error bars. As our final result we take that obtained from Z_a/Z_p, since it has the smallest statistical error.

Then we locate λ^* by studying the scaling corrections to a quantity $\overline{R}$ defined in terms of two dimensionless ratios R_1 and R_2. To define $\overline{R}$, we fix a number $R_{1,f}$ which should be a good approximation to R_1^*; see Ref. 36. Then, for a given value of λ and L, we determine $\beta_f(L,\lambda)$ from

$$R_1(L,\lambda,\beta_f) = R_{1,f}. \tag{3}$$

In our analysis, β_f is determined by taking either $(Z_a/Z_p)_f = 0.1944$ or $(\xi_{2\mathrm{nd}}/L)_f = 0.5644$. Note that β_f approaches β_c as

$$\beta_f = \beta_c + C_f L^{-1/\nu} + \cdots, \tag{4}$$

where the prefactor C_f depends on the choice of $R_{1,f}$. In particular, if $R_{1,f}=R_1^*$, then $C_f=0$ and the leading corrections are proportional to $L^{-1/\nu-\omega}$.

Next we define $\overline{R}$ by

$$\overline{R}(L,\lambda) \equiv R_2(L,\lambda,\beta_f). \tag{5}$$

Here we take either U_4 or U_6 as R_2. Below, we often refer to $\overline{R}$ as R_2 at $R_{1,f}$. Up to subleading corrections, $\overline{R}$ behaves as

$$\overline{R}(L,\lambda) \approx \overline{R}^* + \overline{c}(\lambda) L^{-\omega}. \tag{6}$$

The optimal value λ^* is obtained by solving $\overline{c}(\lambda)=0$. We obtain $\lambda^*=4.6(4)$, 4.7(8), 4.7(8), and 4.6(8) from U_4 at $(Z_a/Z_p)_f=0.1944$, U_4 at $(\xi_{2\mathrm{nd}}/L)_f=0.5644$, U_6 at $(Z_a/Z_p)_f=0.1944$ and U_6 at $(\xi_{2\mathrm{nd}}/L)_f=0.5644$, respectively. As our final result we quote

$$\lambda^* = 4.6(4) \tag{7}$$

from U_4 at $(Z_a/Z_p)_f=0.1944$.

Finally, we compute the critical exponents ν and η using standard FSS methods. Usually, the exponent ν is computed from the slope of a dimensionless ratio R at β_c. Here, following Ref. 42, we replace β_c by β_f, which simplifies the error analysis, and determine ν from the relation

$$\left.\frac{\partial R}{\partial \beta}\right|_{\beta_f} = \overline{a} L^{1/\nu}. \tag{8}$$

TABLE V. Results for β_c at $\lambda=4.0$ and 5.0 using only $L=96$ and the ansatz $R(\beta_c)=R^*$, where R^* is taken from Table IV. In parentheses we give the statistical error, and in brackets the error due to the uncertainty on R^*.

λ	Z_a/Z_p	$\xi_{2\mathrm{nd}}/L$	U_4	U_6
4.0	0.6843895(20)[15]	0.6843887(21)[14]	0.6843898(31)[20]	0.6843898(31)[26]
5.0	0.6875638(21)[16]	0.6875633(26)[15]	0.6875655(34)[20]	0.6875646(34)[26]

We study the derivative of all four quantities U_4, U_6, $\xi_{2\rm nd}/L$, and Z_a/Z_p, and fix β_f by using either $(\xi_{2\rm nd}/L)_f = 0.5644$ or $(Z_a/Z_p)_f = 0.1944$. We arrive at the final estimate

$$\nu = 0.7113(11), \tag{9}$$

where the error includes both the statistical and the systematic uncertainty.

The exponent η is computed from the finite-size behavior of the magnetic susceptibility:

$$\chi|_{\beta_f} = cL^{2-\eta}. \tag{10}$$

In addition, we also use a fit ansatz that includes a constant background term:

$$\chi|_{\beta_f} = cL^{2-\eta} + b. \tag{11}$$

As before, we fix β_f by setting either $(\xi_{2\rm nd}/L)_f = 0.5644$ or $(Z_a/Z_p)_f = 0.1944$. Our final MC estimate is

$$\eta = 0.0378(6). \tag{12}$$

III. CRITICAL EXPONENTS FROM THE IMPROVED HIGH-TEMPERATURE EXPANSION

As shown in the case of the Ising[38] and XY universality classes,[39,36] the analysis of HT expansions for improved Hamiltonians with suppressed leading scaling corrections leads to considerably precise results even for moderately long series. In the present paper, the analysis of 20th-order HT expansions for the improved ϕ^4 lattice Hamiltonian, i.e., for $\lambda \approx \lambda^* = 4.6(4)$, allows us to substantially improve the accuracy of the estimates of the critical exponents. As we shall see, the results turn out to be more precise than those obtained in Sec. II. They also significantly improve those obtained from the analysis of longer series (21 orders) for the standard Heisenberg model (which is recovered in the limit $\lambda \to \infty$) on the cubic and bcc lattices.[40] In this section we report the results of our analyses of the HT series. The details are reported in Appendix B.

We determine γ and ν from the analysis of the HT expansion to $O(\beta^{20})$ of the magnetic susceptibility and of the second-moment correlation length. In Appendix B 2 we report some details and intermediate results, so that the reader can judge the quality of our results without the need of performing his own analysis. They should give an idea of the reliability of our estimates and of the meaning of the errors we quote, which depend on many somewhat arbitrary choices and are therefore partially subjective.

We analyze the HT series by means of integral approximants (IA's) of first, second, and third order. The most precise results are obtained biasing the value of β_c with its MC estimate. We consider several sets of biased IA's, and for each of them we obtain estimates of the critical exponents. These results are reported in Appendix B 2. All sets of IA's give substantially consistent results. Moreover, the results are also stable with respect to the number of terms of the series, so that there is no need to perform problematic extrapolations in the number of terms in order to obtain the final estimates. The error due to the uncertainty on λ^* is estimated by considering the variation of the results when changing the values of λ.

Using the results reported in Appendix B 2 for the analysis at $\lambda = 4.0$, 4.5, and 5.0, we obtain

$$\gamma = 1.39582(10)[18] + 0.0015(\lambda - 4.5), \tag{13}$$

$$\nu = 0.71111(5)[8] + 0.0009(\lambda - 4.5). \tag{14}$$

The number between parentheses is basically the spread of the approximants at $\lambda = 4.5$ using the central value of β_c, while the number between brackets gives the systematic error due to the uncertainty on β_c. Equations (13) and (14) also show the dependence of the results on the chosen value of λ. The λ dependence is estimated by using the results for $\lambda = 4.0$ and $\lambda = 5.0$.

Using the MC estimate $\lambda^* = 4.6(4)$, we obtain

$$\gamma = 1.39597(10)[18]\{60\}, \tag{15}$$

$$\nu = 0.71120(5)[8]\{36\}, \tag{16}$$

where the error due to the uncertainty on λ^* is reported between braces. Thus our final estimates are

$$\gamma = 1.3960(9), \tag{17}$$

$$\nu = 0.7112(5), \tag{18}$$

where the uncertainty is estimated by summing the three errors reported above.

Using the above-reported results for γ and ν and the scaling relation $\gamma = (2-\eta)\nu$, we obtain $\eta = 0.037(2)$, where the error is estimated by considering the errors on γ and ν as independent, which is of course not true. We can obtain an estimate of η with a smaller, yet reliable, error by applying the so-called critical-point renormalization method[67] to the series of χ and ξ^2. This method provides an estimate for the combination $\eta\nu$. Proceeding as before, we obtain

$$\eta\nu = 0.02665(18) + 0.00035(\lambda - 4.5). \tag{19}$$

Taking into account that $\lambda^* = 4.6(4)$, we find

$$\eta\nu = 0.02669(18)[14], \tag{20}$$

where the first error is related to the spread of the IA's and the second one to the uncertainty on λ^*, evaluated as before. Thus

$$\eta = 0.0375(3)[2]. \tag{21}$$

Moreover, using the scaling relations, one obtains

$$\alpha = 2 - 3\nu = -0.1336(15), \tag{22}$$

$$\delta = \frac{5-\eta}{1+\eta} = 4.783(3), \tag{23}$$

$$\beta = \frac{\nu}{2}(1+\eta) = 0.3689(3), \tag{24}$$

where the error of β has been estimated by considering the errors of ν and η as independent.

IV. CRITICAL EQUATION OF STATE

In this section we determine the critical equation of state characterizing the Heisenberg universality class. The critical equation of state relates the thermodynamical quantities in the neighborhood of the critical temperature, in both phases. It is usually written in the form

$$\vec{H}=(B_c)^{-\delta}\vec{M}M^{\delta-1}f(x), \tag{25}$$

$$x\equiv t(M/B)^{-1/\beta}, \tag{26}$$

where $f(x)$ is a universal scaling function normalized in such a way that $f(-1)=0$ and $f(0)=1$, and B_c and B are the amplitudes of the magnetization on the critical isotherm and on the coexistence curve:

$$M=B_cH^{1/\delta}, \quad t=0, \tag{27}$$

$$M=B(-t)^{\beta}, \quad H=0, \ t<0. \tag{28}$$

Griffiths' analyticity implies that $f(x)$ is regular everywhere for $x>-1$. It has a regular expansion in powers of x,

$$f(x)=1+\sum_{n=1}^{\infty} f_n^0 x^n, \tag{29}$$

and a large-x expansion of the form

$$f(x)=x^{\gamma}\sum_{n=0}^{\infty} f_n^{\infty} x^{-2n\beta}. \tag{30}$$

Moreover, at the coexistence curve, i.e., for $x\to -1$,[68–72]

$$f(x)\approx c_f(1+x)^2. \tag{31}$$

The nature of the corrections to the leading behavior at the coexistence curve is less clear, see, e.g., Refs. 70–73, and 56. From the scaling function $f(x)$ one may derive many interesting universal amplitude ratios involving zero-momentum quantities, such as specific heat, magnetic susceptibility, etc. For example, the universal ratio U_0 of the specific-heat amplitudes in the two phases can be written as (see, e.g., Ref. 74)

$$U_0\equiv\frac{A^+}{A^-}=\frac{\varphi(\infty)}{\varphi(-1)}, \tag{32}$$

where, in the Heisenberg case for which $-1<\alpha<0$,

$$\varphi(x)=\frac{x|x|^{\alpha-2}f'(0)}{\alpha-1}+\frac{|x|^{\alpha}f''(0)}{\alpha}-|x|^{\alpha-2}f(x) + \int_0^x dy|y|^{\alpha-2}[f'(y)-f'(0)-yf''(0)]. \tag{33}$$

We mention that the critical equation of state for the N-vector model has been computed to $O(\epsilon^2)$ in the framework of the ϵ-expansion[75] and to $O(1/N)$ in the framework of the $1/N$ expansion.[68]

As our starting point for the determination of the critical equation of state, we determine the first few nontrivial coefficients of its small-magnetization expansion, by analyzing the corresponding HT series for the improved ϕ^4 Hamiltonian. These results are then used to construct parametric representations of the critical equation of state which are valid in the whole critical region. Then, from our approximate representations of the equation of state we derive estimates of several universal amplitude ratios. This method was already applied to the Ising universality class in three[76,38] and two dimensions,[77] and to the three-dimensional XY universality class.[78,36]

A. Small-magnetization expansion of the Helmholtz free energy

We write the Helmholtz free energy as[76,79]

$$\Delta\mathcal{F}=\mathcal{F}(M)-\mathcal{F}_{\rm reg}(M)=\frac{m^3}{g_4}A(z), \tag{34}$$

where $m=1/\xi$, ξ is the second-moment correlation length, g_4 is the zero-momentum four-point coupling, and

$$z\equiv k|M|t^{-\beta}, \tag{35}$$

where k is an appropriate amplitude ratio. The small-magnetization expansion of the free energy corresponds to the small-z expansion of $A(z)$,

$$A(z)=\frac{1}{2}z^2+\frac{1}{4!}z^4+\sum_{j=3}\frac{1}{(2j)!}r_{2j}z^{2j}, \tag{36}$$

which also fixes the normalization k of z. Correspondingly, for the equation of state we obtain

$$\vec{H}=\frac{\partial\mathcal{F}(M)}{\partial\vec{M}}\propto\frac{\vec{M}}{|M|}t^{\beta\delta}F(z), \tag{37}$$

with $F(z)\equiv\partial A/\partial z$. Because of Griffiths' analyticity, $\mathcal{F}(M)$ has a regular expansion in powers of t for $|M|$ fixed. Therefore, $F(z)$ has the large-z expansion

$$F(z)=z^{\delta}\sum_{k=0} F_k^{\infty} z^{-k/\beta}. \tag{38}$$

The function $F(z)$ is defined only for $t>0$. For $t<0$ the equation of state is expressed in terms of a different function which is however analytically related to $F(z)$ since the free energy and the equation of state are analytic on the critical isotherm $t=0$ for $H\neq 0$. The two functions $f(x)$ and $F(z)$ are clearly related,

$$z^{-\delta}F(z)=F_0^{\infty}f(x), \quad z=z_0x^{-\beta}, \tag{39}$$

where $z_0=kB$.

In order to estimate the universal quantities g_4 and r_{2j} from the corresponding improved HT expansions (see Ap-

TABLE VI. Estimates of g_4, r_6, and r_8, obtained using various approaches.

	IHT	HT	$d=3$ exp.	ϵ-exp.	CRG
g_4	19.13(10)	19.31(14), 19.27(11) (Ref. 80) 19.34(16) (Ref. 82)	19.06(5) (Ref. 47) 19.06 (Ref. 48)	19.55(12) (Refs. 81 and 82)	22.35 (Refs. 55 and 64)
r_6	1.86(4)	2.1(6) (Ref. 83)	1.880 (Ref. 84) 1.884(32) (Ref. 81)	1.867(9) (Refs. 81 and 85)	1.74 (Ref. 86)
r_8	0.6(2)		0.975 (Ref. 84)	1.0(6) (Refs. 81 and 85)	0.84 (Ref. 86)

pendix B 1), we essentially used the analysis described in Ref. 36. Here we report only the final estimates

$$g_4 = 19.13(8)[2], \tag{40}$$

$$r_6 = 1.86(3)[1], \tag{41}$$

$$r_8 = 0.60(15)[5], \tag{42}$$

where the error in parentheses is related to the spread of the approximants and the second one in brackets to the uncertainty on λ^*, evaluated as before. Moreover, we obtained the rough estimate $r_{10} = -15(10)$. In Table VI we compare our results (denoted by IHT) with the estimates obtained using other approaches, such as HT expansions for the standard $O(3)$-vector model (HT), field-theoretical fixed-dimension perturbative expansions ($d=3$ exp.), ϵ expansions (ϵ-exp.), and approximate solutions of continuous renormalization-group equations (CRG). All estimates are in good agreement, Only the ϵ-expansion estimate of g_4 is significantly higher than the IHT estimate (as already noted in Ref. 81, the error may be underestimated). The CRG estimates are much less precise than the results of other methods.

B. Parametric representations of the equation of state

In order to obtain approximations of the equation of state valid in the whole critical region, we use parametric representations that implement the expected scaling and analytic properties. We write[87–89]

$$M = m_0 R^\beta m(\theta),$$

$$t = R(1-\theta^2),$$

$$H = h_0 R^{\beta\delta} h(\theta), \tag{43}$$

where h_0 and m_0 are normalization constants. The variable R is non-negative, and measures the distance from the critical point in the (t,H) plane, while the variable θ parametrizes the displacement along the lines of constant R. The functions $m(\theta)$ and $h(\theta)$ are odd and normalized so that $m(\theta)=\theta+O(\theta^3)$ and $h(\theta)=\theta+O(\theta^3)$. The smallest positive zero of $h(\theta)$, which should satisfy $\theta_0>1$, corresponds to the coexistence curve, i.e., to $T<T_c$ and $H\to 0$. The parametric representation satisfies the requirements of regularity of the equation of state. Singularities can appear only at the coexistence curve (due, for example, to the logarithms discussed in Ref. 73), i.e., for $\theta=\theta_0$. Mapping (43) is not invertible when its Jacobian vanishes, which occurs when

$$Y(\theta) \equiv (1-\theta^2)m'(\theta) + 2\beta\theta m(\theta) = 0. \tag{44}$$

Thus parametric representations based on mapping (43) are acceptable only if $\theta_0 < \theta_l$ where θ_l is the smallest positive zero of the function $Y(\theta)$.

The functions $m(\theta)$ and $h(\theta)$ are related to the scaling function $f(x)$ through

$$x = \frac{1-\theta^2}{\theta_0^2-1}\left[\frac{m(\theta_0)}{m(\theta)}\right]^{1/\beta},$$

$$f(x) = \left[\frac{m(\theta)}{m(1)}\right]^{-\delta}\frac{h(\theta)}{h(1)}. \tag{45}$$

The asymptotic behavior [Eq. (31)] is reproduced simply by requiring that

$$h(\theta) \sim (\theta_0-\theta)^2 \quad \text{for} \quad \theta\to\theta_0. \tag{46}$$

The scaling function $F(z)$ is obtained by

$$z = \rho\, m(\theta)(1-\theta^2)^{-\beta},$$

$$F(z(\theta)) = \rho(1-\theta^2)^{-\beta\delta}h(\theta), \tag{47}$$

where ρ may be taken as a free parameter.[76,38,78,56]

C. Approximate polynomial representations

Following Ref. 78, we construct approximate polynomial parametric representations that have the expected singular behavior at the coexistence curve (Goldstone singularity) and match the known terms of the small-z expansion of $F(z)$ [cf. Eqs. (36) and (37)]. We consider two distinct approximation schemes. In the first one, which we denote by A, $h(\theta)$ is a polynomial of fifth order with a double zero at θ_0, and $m(\theta)$ is a polynomial of order $(1+2n)$:

$$\text{scheme A:} \quad m(\theta) = \theta\left(1+\sum_{i=1}^{n} c_i\theta^{2i}\right),$$

$$h(\theta) = \theta(1-\theta^2/\theta_0^2)^2. \tag{48}$$

In the second scheme, denoted by B, we set

$$\text{scheme B:} \quad m(\theta) = \theta,$$

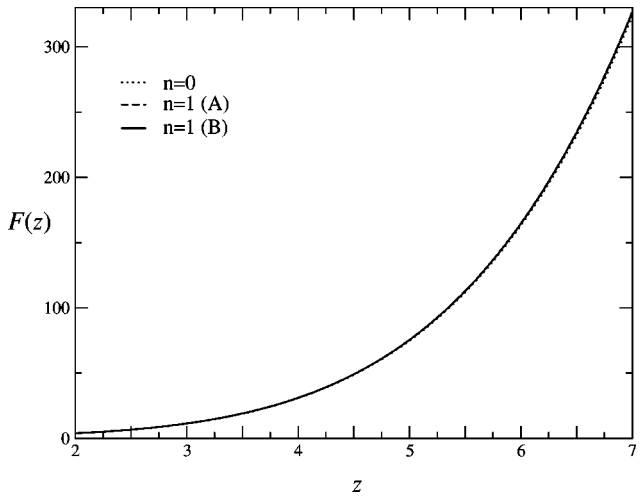

FIG. 1. The scaling function $F(z)$ vs z.

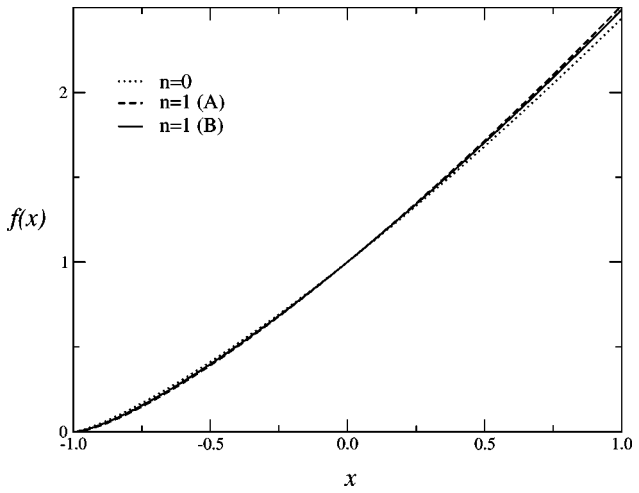

FIG. 2. The scaling function $f(x)$ vs x.

$$h(\theta)=\theta(1-\theta^2/\theta_0^2)^2\left(1+\sum_{i=1}^{n} c_i\theta^{2i}\right). \tag{49}$$

Here $h(\theta)$ is a polynomial of order $5+2n$ with a double zero at θ_0. For $n=0$ the approximations A and B coincide. Note that, for scheme B,

$$Y(\theta)=1-\theta^2+2\beta\theta^2, \tag{50}$$

independently of n, so that $\theta_l=(1-2\beta)^{-1}$. In both schemes, ρ, θ_0, and the n coefficients c_i are determined by matching the small-z expansion of $F(z)$. Thus, in order to fix the n coefficients c_i we use $n+1$ values of r_{2j}, i.e., $r_6, \ldots r_{6+2n}$.

As input parameters for our analysis we consider the estimates $\alpha=-0.1336(15)$, $\eta=0.0375(5)$, $r_6=1.86(4)$, and $r_8=0.6(2)$, which are the results of our HT analysis. The available estimate of r_{10} is too imprecise for our purposes. In Fig. 1 we show the curves obtained in schemes A and B with $n=0,1$ and for $\alpha=-0.1336$, $\eta=0.0375$, $r_6=1.86$, and $r_8=0.6$. The differences among the three approximations should give an indication of the uncertainty. The three approximations of $F(z)$ are practically indistinguishable, and differ at most by approximately 2% (the difference between the two $n=1$ curves is much smaller). Thus, by using the first two coefficients r_{2j}, one obtains reasonably precise approximations of the scaling function $F(z)$ for all positive values of z, i.e., for the whole HT phase up to $t=0$. This is also numerically confirmed by the estimates of the universal constant F_0^∞, cf. Eq. (38), which is related to the large-z behavior of $F(z)$. Indeed, we obtain $F_0^\infty=0.0262(4)$, 0.0266(5), 0.0266(5) respectively for $n=0$, $n=1$ (scheme A), and $n=1$ (scheme B), where the reported errors refer only to the uncertainty of the input parameters. This fact is not trivial, since the small-z expansion has a finite convergence radius.[90] Therefore, the determination of $F(z)$ on the whole positive real axis from its small-z expansion requires an analytical continuation, which turns out to be effectively performed by the approximate parametric representations we have considered.

In Fig. 2 we plot the approximations of $f(x)$ corresponding to the schemes A and B for $n=0,1$, using the central values of the input parameters. The three curves are in substantial agreement, especially those with $n=1$. Indeed, the difference between them is within the uncertainty due to the errors on the input parameters. These approximate parametric representations are not precise at the coexistence curve; indeed, as we shall see, the estimates of c_f [cf. Eq. (31),] are rather imprecise and very sensitive to the value of r_8, which is not known with high precision. We mention that in Ref. 55 an approximate expression for $f(x)$ was obtained by approximately solving the continuous renormalization-group equations for the free energy (average action). The results are quite imprecise, as we shall show later by comparing the corresponding estimates for some universal amplitude ratios.

D. Universal amplitude ratios

From the critical equation of state one may derive estimates of several universal amplitude ratios. They are expressed in terms of the amplitudes of the magnetization [cf. Eqs. (27) and (28)], of the singular part of the specific heat,

$$C_{H,\mathrm{sing}}=A^{\pm}|t|^{-\alpha}, \tag{51}$$

of the magnetic susceptibility in the HT phase,

$$\chi=NC^{+}t^{-\gamma}, \tag{52}$$

of the zero-momentum four-point connected correlation function in the HT phase,

$$\chi_4=\frac{N(N+2)}{3}C_4^{+}t^{-\gamma-2\beta\delta}, \tag{53}$$

and of the second-moment correlation length in the HT phase,

$$\xi=f^{+}t^{-\nu}, \tag{54}$$

where $N=3$. We also consider the crossover (or pseudocritical) line $t_{\max}(H)$, that is defined as the reduced temperature

for which the longitudinal magnetic susceptibility $\chi_L(t,H) = \partial M/\partial H$ has a maximum at H fixed. The renormalization group predicts

$$t_{\max}(H) = T_p H^{1/(\gamma+\beta)}, \tag{55}$$

$$\chi_L(t_{\max}, H) = C_p t_{\max}^{-\gamma}. \tag{56}$$

We consider several universal amplitude ratios:

$$U_0 \equiv \frac{A^+}{A^-}, \tag{57}$$

$$R_\chi \equiv \frac{C^+ B^{\delta-1}}{(B_c)^\delta}, \tag{58}$$

$$R_C \equiv \frac{\alpha A^+ C^+}{B^2}, \tag{59}$$

$$R_4 \equiv -\frac{C_4^+ B^2}{(C^+)^3}, \tag{60}$$

$$R_\xi^+ \equiv (\alpha A^+)^{1/3} f^+ = \left(\frac{R_C R_4}{g_4}\right)^{1/3}, \tag{61}$$

$$P_m \equiv \frac{T_p^\beta B}{B_c}, \tag{62}$$

$$P_c \equiv -\frac{T_p^{2\beta\delta} C^+}{C_4^+} = \frac{P_m^{2\delta}}{R_\chi^2 R_4}, \tag{63}$$

$$R_p \equiv \frac{C^+}{C_p}. \tag{64}$$

Morever, we estimate

$$R_\alpha \equiv \frac{1-U_0}{\alpha}, \tag{65}$$

which, as suggested in Ref. 74, should be less sensitive to the value of α than U_0. In Appendix C we give their expressions in terms of the functions $m(\theta)$ and $h(\theta)$.

In Table VII we report the universal amplitude ratios, as derived by the approximate polynomial representations of the equation of state for $n=0$ and 1. The reported errors are only due to the uncertainty of the input parameters and do not include the systematic error of the procedure, which may be determined by comparing the results of the various approximations. In Table VII we also show results for $z_{\max}$, $x_{\max}$, and $w_{\max}$ which are the values of the scaling variable z, x, and w [w will be defined in Eq. (71)] associated with the crossover line, F_0^∞ [cf. Eq. (38)], which is related to the large-z behavior of $F(z)$, r_8, and r_{10} [cf. Eqs. (36) and (37)], which are related to the small-z expansion of $F(z)$, f_1^0, f_2^0, and f_3^0 [cf. Eq. (29)], which are related to the expansion at $x=0$ of $f(x)$, and c_f [cf. Eq. (31)], which is related to the behavior at the coexistence curve. Note that $f_0^\infty = R_\chi^{-1}$ where f_0^∞ is related to the large-x behavior of $f(x)$ [cf. Eq. (30)].

TABLE VII. Results for the parameters and the universal amplitude ratios using the scheme A [cf. Eq. (48)], and scheme B [cf. Eq. (49)]. Note that the quantities reported in the first three lines do not have a physical meaning, but are related to the particular parametric representation employed. Numbers marked with an asterisk are inputs, not predictions.

	$n=0$	$n=1$ A	$n=1$ B
ρ	2.14(2)	2.20(4)	2.08(4)
θ_0^2	3.81(1)	3.3(1)	2.7(2)
c_1	0	−0.016(9)	0.055(20)
U_0	1.61(2)	1.56(3)	1.57(3)
R_α	4.6(2)	4.2(3)	4.3(2)
R_χ	1.41(2)	1.28(8)	1.33(4)
R_C	0.173(3)	0.19(1)	0.184(6)
R_4	8.2(2)	7.7(3)	7.9(2)
R_ξ^+	0.421(1)	0.425(3)	0.423(2)
P_m	1.201(5)	1.17(2)	1.18(1)
P_c	0.354(4)	0.357(5)	0.357(5)
R_p	2.026(6)	2.020(5)	2.021(7)
$z_{\max}$	1.278(5)	1.275(5)	1.275(6)
$x_{\max}$	8.9(1)	8.3(4)	8.5(2)
$w_{\max}$	1.64(2)	1.53(6)	1.57(4)
F_0^∞	0.0262(4)	0.0266(5)	0.0266(5)
r_8	0.23(5)	*0.6(2)	*0.6(2)
r_{10}	−1.1(3)	−6(2)	−7(3)
f_1^0	1.28(1)	1.36(5)	1.33(3)
f_2^0	0.181(5)	0.21(2)	0.20(1)
f_3^0	−0.102(1)	−0.105(2)	−0.094(5)
c_f	22(5)	5(3)	8(3)

From the results of Table VII we arrive at the final estimates denoted by IHT–PR in Table VIII, obtained by taking the weighted average of the results for $n=1$. The error we quote is the sum of the uncertainty induced by the error on the input parameters and of one-half of the difference between the two approximations with $n=1$. In most cases these estimates include the results of the $n=0$ approximation. In Table VIII we compare our results with those obtained in other approaches and in experiments.[101] We mention that the field-theoretical estimates of U_0 have been obtained from the analysis of the fixed-dimension expansion in the framework of the minimal renormalization without ϵ expansion,[91,93] and from the standard ϵ expansion to $O(\epsilon^2)$.[92] The estimate of U_0 by CRG was obtained using Eq. (33) and the approximate expression for $f(x)$ reported in Refs. 55 and 64. See, e.g., Ref. 102 for a more complete review of theoretical and experimental estimates of universal amplitude ratios.

In addition, from the approximate parametric representations of the equation of state, we obtain the estimates

$$f_1^0 = 1.34(5),$$

$$f_2^0 = 0.20(2),$$

TABLE VIII. Estimates of universal amplitude ratios obtained using different approaches. The numbers marked by asterisks were obtained by us using the results reported in the corresponding references.

	IHT–PR	$d=3$ exp.	ϵ-exp.	CRG	HT	Experiments
U_0	1.56(4)	1.51(4) (Ref. 91) 1.544 (Ref. 93)	1.521(22) (Ref. 92)	*1.823 (Refs. 55 and 64)		1.50(5) (Ref. 17) 1.27(9) (Ref. 29) 1.4(4) (Ref. 94)
R_α	4.3(3)	*4.4(4) (Ref. 91) *4.46 (Ref. 93)	4.56(9) (Ref. 92)	*3.41 (Refs. 55 and 64)		
R_χ	1.31(7)		1.33 (Ref. 95)	1.11 (Refs. 55 and 64)		
R_C	0.185(10)	0.189(9) (Ref. 96) 0.194 (Ref. 93)	0.17 (Ref. 97)			
R_4	7.8(3)					
R_ξ^+	0.424(3)	0.4347(20) (Ref. 98) 0.4319(17) (Ref. 100)	0.42 (Ref. 99)		0.431(5) (Ref. 65) 0.433(5) (Ref. 65)	

$$f_3^0 = -0.10(1),$$

$$F_0^\infty = 0.0266(5),$$

$$r_{10} = -6(3). \tag{66}$$

The estimate of r_{10} should be compared with the much less precise HT result $r_{10}=-15(10)$ obtained in Sec. IV A. Concerning the quantities involving amplitudes at the crossover line, we report the estimates

$$P_m = 1.18(2), \tag{67}$$

$$P_c = 0.357(5), \tag{68}$$

$$R_p = 2.020(6), \tag{69}$$

$$z_{\max} = 1.275(5). \tag{70}$$

In order to determine the behavior of the longitudinal magnetic susceptibility $\chi_L = \partial M/\partial H$ as a function of t and H, one may consider the scaling function

$$D(w) \equiv B_c^{-1} H^{1-1/\delta} \chi_L = \frac{f(x)^{1-1/\delta}}{\delta f(x) - \frac{1}{\beta} x f'(x)},$$

$$w \equiv (B/B_c)^{1/\beta} t H^{-1/(\beta\delta)} = x f(x)^{-1/(\beta\delta)}. \tag{71}$$

The function $D(w)$ has a maximum for $w_{\max}=1.55(6)$. In order to simplify possible comparisons, it is convenient to consider the rescaled function

$$C(u) = \frac{D(w)}{D(w_{\max})},$$

$$u = \frac{w}{w_{\max}}, \tag{72}$$

which is such that the maximum corresponds to $u=1$ and satisfies $C(1)=1$. In Fig. 3 we plot the scaling function $C(u)$ versus u, as obtained from the $n=0,1$ approximate parametric representations.

E. Comparison with the experiments

In spite of the large number of experiments, at present there is no accurate quantitative study of the equation of state in the critical regime. Here we shall discuss three different representations that are widely used in the experimental work, and we shall give explicit formulas for them.

A first possibility[103] consists in studying the behavior of $h/m \equiv H|t|^{-\gamma}/M$ versus $m^2 = M^2|t|^{-2\beta}$. Such a function can be easily obtained from our approximations for $f(x)$, since $m^2 = B^2|x|^{-2\beta}$ and

$$\frac{h}{m} = k|x|^{-\gamma} f(x) \tag{73}$$

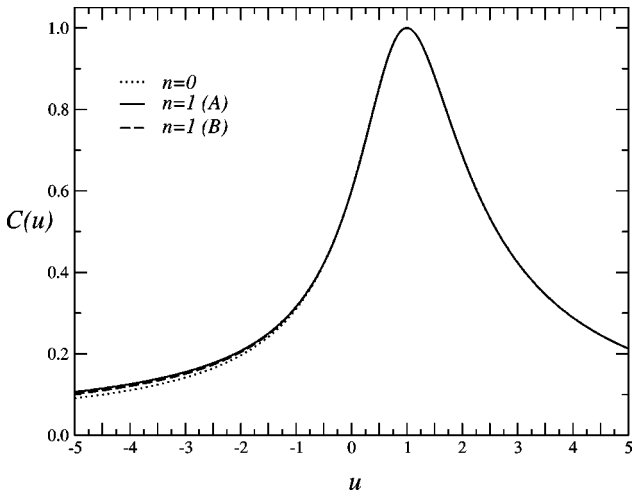

FIG. 3. The scaling function $C(u)$ [cf. Eqs. (72) and (71)].

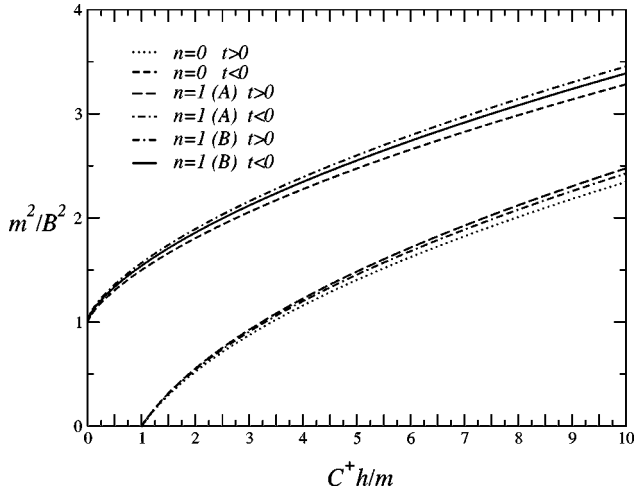

FIG. 4. Plot of m^2/B^2 vs C^+h/m.

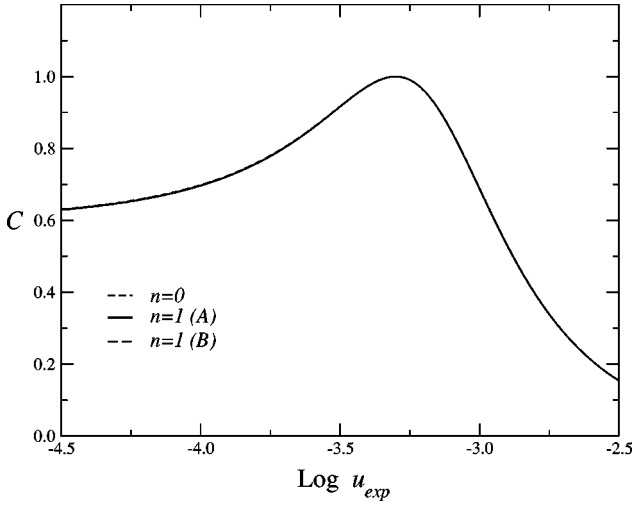

FIG. 5. The scaling function $C(u)$ vs the experimental scaling variable $u_{\rm expt} \equiv tH^{-1/(\beta\delta)}$.

where the constant k can be written as

$$k=(B_c)^{-\delta}B^{\gamma/\beta}=\frac{R_\chi}{C^+}. \tag{74}$$

The universal ratio R_χ has been computed in the previous section, $R_\chi=1.31(7)$, and B and B_c are nonuniversal amplitudes defined in Eqs. (28) and (27). A plot of m^2/B^2 versus C^+h/m is reported in Fig. 4. It agrees qualitatively with the analogous experimental ones reported, e.g., in Refs. 17, 20, and 104. Often, for small h/m one approximates the equation of state by writing

$$\frac{h}{m}=a_\pm+b_\pm m^2, \tag{75}$$

where $a_\pm$ and $b_\pm$ are numerical coefficients depending on the phase. Such an approximation has a very limited range of validity. In the HT phase, we obtain, for $m^2\to 0$,

$$\begin{aligned}\frac{h}{m}&=\frac{1}{C^+}\left[1+\frac{R_4}{6}\frac{m^2}{B^2}+\sum_{n=2}^{\infty}\frac{R_4^n r_{2n+2}}{(2n+1)!}\left(\frac{m^2}{B^2}\right)^n\right]\\ &\approx\frac{1}{C^+}\left[1+1.30(5)\frac{m^2}{B^2}+0.94(8)\left(\frac{m^2}{B^2}\right)^2\right.\\ &\quad\left.+0.06(2)\left(\frac{m^2}{B^2}\right)^3+\cdots\right],\end{aligned} \tag{76}$$

where we have used the estimate of R_4 reported in Table VIII, and the estimates of r_6 and r_8 reported in Table VI. From Eq. (76) we see that approximation (75) is valid only for very small m^2, i.e., at the 1% level only for $m^2 \lesssim 0.01B^2$. The quadratic approximation—i.e. the approximation with an additional $(m^2)^2$ term—has a much wider range of validity because of the smallness of the coefficient of m^6.

In the low-temperature phase, Eq. (75) is theoretically incorrect, since for $m^2/B^2\to 1$ we have

$$\frac{h}{m}\approx\frac{kc_f}{4\beta^2}\left(1-\frac{m^2}{B^2}\right)^2, \tag{77}$$

where c_f is defined in Eq. (31) and can be estimated roughly from the results reported in Table VII. Equation (77) is inconsistent with approximation (75) near the coexistence curve, due to the presence of Goldstone modes. It would be correct only in Ising systems.

Finally, note that for m^2 large we have

$$\frac{h}{m}\approx k\left(\frac{m}{B}\right)^{\delta-1}. \tag{78}$$

A second form that is widely used to analyze the experimental data is the Arrott-Noakes[105] scaling equation

$$\left(\frac{H}{M}\right)^{1/\gamma}=at+bM^{1/\beta}, \tag{79}$$

where a and b are numerical constants. This approximation is good in a neighborhood of the critical isotherm $t=0$. Since

$$\left(\frac{H}{M}\right)^{1/\gamma}k^{-1/\gamma}=\left(\frac{M}{B}\right)^{1/\beta}f(x)^{1/\gamma}, \tag{80}$$

using Eq. (29) and the numerical values reported in Eq. (66), we obtain

$$\begin{aligned}\left(\frac{H}{M}\right)^{1/\gamma}k^{-1/\gamma}&=\left(\frac{M}{B}\right)^{1/\beta}+0.96(4)t-0.04(2)t^2\left(\frac{M}{B}\right)^{-1/\beta}\\ &\quad-0.02(2)t^3\left(\frac{M}{B}\right)^{-2/\beta}\cdots.\end{aligned} \tag{81}$$

Thus, at a 1% level of precision the Arrott-Noakes formula is valid approximately for $t(MB^{-1})^{-1/\beta}\lesssim 25$ which is quite a large interval.

Finally, Ref. 6 reported an experimental study of the behavior of the critical system at the crossover line, and showed a plot of the curve $C(u)$ [cf. Eq. (72)], in terms of the unnormalized variable $u_{\rm expt}\equiv tH^{-1/(\beta\delta)}$. We can attempt a quantitative comparison with the results reported in their Fig. 4. For this purpose, in Fig. 5 we plot $C(u)$ in terms of their variable for the range of $u_{\rm expt}$ accessible to the experiment.[106]

A direct comparison of this figure with Fig. 4 of Ref. 6 shows a very nice quantitative agreement.

APPENDIX A: MONTE CARLO SIMULATIONS

In this appendix we present some details of the analyses of the MC data. Details on the simulation can be found in Ref. 37.

1. Definitions

In all our work, considerable importance is played by dimensionless ratios (or phenomenological couplings) R. In order to have better control on systematic errors we have studied four dimensionless ratios. We first consider the Binder cumulant U_4,[107] and its generalization U_6 defined by

$$U_{2j}=\frac{\langle(\vec{m}^2)^j\rangle}{\langle\vec{m}^2\rangle^j}, \tag{A1}$$

where

$$\vec{m}=\frac{1}{V}\sum_x \vec{\phi}_x \tag{A2}$$

is the magnetization of the system. The third quantity that we studied is the second-moment correlation length divided by the linear extension of the lattice $\xi_{2\mathrm{nd}}/L$. The second-moment correlation length is defined by

$$\xi_{2\mathrm{nd}}=\sqrt{\frac{\chi/F-1}{4\sin(\pi/L)^2}}, \tag{A3}$$

where

$$\chi=\frac{1}{V}\left\langle\left(\sum_x \vec{\phi}_x\right)^2\right\rangle \tag{A4}$$

is the magnetic susceptibility and

$$F=\frac{1}{V}\left\langle\left|\sum_x \exp\left(i\frac{2\pi x_1}{L}\right)\vec{\phi}_x\right|^2\right\rangle \tag{A5}$$

is the Fourier transform of the two-point correlation function at the lowest nonvanishing momentum. In order to reduce the statistical error, we averaged the results of all three directions of the lattice.

The fourth quantity is the ratio Z_a/Z_p, where Z_a is the partition function with antiperiodic boundary conditions in one of the three directions and Z_p the corresponding one with periodic boundary conditions in all directions. Antiperiodic boundary conditions mean that the term $\Sigma_{\langle xy\rangle}\vec{\phi}_x\cdot\vec{\phi}_y$ in the Hamiltonian is multiplied by -1 for $x=(L_1,x_2,x_3)$ and $y=(1,x_2,x_3)$. This ratio can be measured with the help of a variant of the cluster algorithm, the boundary-flip algorithm. It was introduced in Ref. 108 for the Ising model and generalized to $O(N)$-invariant nonlinear σ models in Ref. 109. As in Refs. 33 and 36, we use a version of the algorithm that only measures Z_a/Z_p and does not perform the flip to antiperiodic boundary conditions. For a recent discussion of the algorithm, see Ref. 36.

TABLE IX. Fits with ansatz (2) of our data for Z_a/Z_p at $\lambda=4.5$. We included all data with $L_{\min}\leqslant L\leqslant L_{\max}$ in the fit.

$L_{\min}$	$L_{\max}$	χ^2/d.o.f.	β_c	$(Z_a/Z_p)^*$
12	96	5.75	0.6862428(6)	0.19408(3)
14	96	1.90	0.6862413(7)	0.19419(3)
16	96	1.29	0.6862406(7)	0.19424(4)
18	96	0.62	0.6862400(7)	0.19430(4)
20	96	0.68	0.6862400(8)	0.19430(5)
22	96	0.75	0.6862400(8)	0.19430(6)
24	96	0.81	0.6862397(10)	0.19434(8)
28	96	0.60	0.6862390(10)	0.19443(10)
12	48	5.96	0.6862459(10)	0.19399(4)
14	48	1.92	0.6862432(10)	0.19413(4)

2. Determination of R^*

First, we compute β_c and the fixed-point value of the dimensionless ratios R^* for $\lambda=4.5$—our best approximation to λ^*—using the standard cumulant crossing method of Binder. For $\lambda=4.5$ we solve Eq. (2), computing $R(L,\beta)$ by using its Taylor expansion up to the third order:

$$R(L,\beta)=R(L,\beta_s)+d_1(L,\beta_s)(\beta-\beta_s)+\frac{1}{2}d_2(L,\beta_s)(\beta-\beta_s)^2+\frac{1}{6}d_3(L,\beta_s)(\beta-\beta_s)^3. \tag{A6}$$

Here β_s is the value of β at which the simulation was performed, and R, d_1, d_2, and d_3 are determined in the MC simulation.

As an example, results for Z_a/Z_p are given in Table IX. In the fits, we include all data with $L_{\min}\leqslant L\leqslant L_{\max}$. For $L_{\max}$ only measures Z_a/Z_p and does not perform the flip to antiperiodic boundary conditions. For a recent discussion of the algorithm, see Ref. 36.

TABLE X. Estimates of $\overline{R}^*$ and $\overline{c}(4.5)$ from the fit (6) of U_4 at $(Z_a/Z_p)_f=0.1944$. Here $\lambda=4.5$.

$L_{\min}$	$L_{\max}$	χ^2/d.o.f.	$\overline{R}^*$	$\overline{c}(4.5)$
6	96	7.87	1.13931(2)	0.00073(12)
8	96	1.71	1.13944(2)	−0.00036(17)
10	96	1.82	1.13942(3)	−0.00022(25)
12	96	1.65	1.13937(4)	0.00039(36)
14	96	1.25	1.13930(5)	0.00118(47)
16	96	1.33	1.13932(5)	0.00097(60)
18	96	1.33	1.13928(6)	0.00145(73)
20	96	1.27	1.13923(7)	0.00217(89)
24	96	1.54	1.13920(10)	0.00273(155)
8	32	1.00	1.13947(3)	−0.00060(19)
8	48	1.26	1.13945(2)	−0.00045(18)
12	48	1.20	1.13939(4)	0.00018(38)
16	48	0.75	1.13936(6)	0.00056(67)

TABLE XI. Estimates of $\overline{R}^*$ and $\overline{c}(4.5)$ from the fit (6) of U_4 at $(\xi_{2\mathrm{nd}}/L)_f=0.5644$. Here $\lambda=4.5$.

$L_{\min}$	$L_{\max}$	χ^2/d.o.f.	$\overline{R}^*$	$\overline{c}(4.5)$
8	96	9.98	1.13984(2)	−0.00493(19)
10	96	5.05	1.13966(3)	−0.00313(31)
12	96	2.32	1.13948(4)	−0.00120(39)
14	96	1.30	1.13937(5)	0.00010(51)
16	96	1.40	1.13936(6)	0.00022(65)
18	96	1.21	1.13929(7)	0.00112(81)
20	96	1.24	1.13925(8)	0.00167(99)
24	96	1.50	1.13923(11)	0.00209(173)
8	48	10.41	1.13987(3)	−0.00514(19)
12	48	1.99	1.13952(4)	−0.00153(42)

$=96$, χ^2/d.o.f. (d.o.f. is the number of degrees of freedom of the fit) is smaller than 1 starting from $L_{\min}=16$. Moreover, the result for β_c is stable when further data are discarded. To be on the safe side, we take our final estimate from the fit with $L_{\min}=28$ and $L_{\max}=96$.

The systematic error due to corrections to scaling is estimated by comparing the results corresponding to $L_{\min}=28$ and $L_{\max}=96$ with those with $L_{\min}=14$ and $L_{\max}=48$. We suppose that the error of β_c is proportional to $L^{-1/\nu-\omega}\approx L^{-2.2}$, where we assume pessimistically leading and not subleading corrections. Hence, we estimate the error on our final result as the difference between the $L_{\min}=28$, $L_{\max}=96$ result and the $L_{\min}=14$, $L_{\max}=48$ result multiplied by $2^{-2.2}/(1-2^{-2.2})$. The systematic error of $(Z_a/Z_p)^*$ is estimated in a similar fashion, assuming that the error is proportional to $L^{-\omega}$.

In the same way we analyze our data for the remaining three dimensionless ratios. Our results are reported in Table IV. Note that the four results for β_c are consistent within error bars. The statistical error of β_c obtained from Z_a/Z_p and $\xi_{2\mathrm{nd}}/L$ is considerably smaller than that from U_4 and U_6. As our final estimate we take $\beta_c=0.6862385(20)$, which is consistent with all four results.

3. Determination of λ^*

In order to compute λ^* we solve the equation $\overline{c}(\lambda)=0$, where $\overline{c}(\lambda)$ is defined in Eq. (6). In practice, we replace $\overline{c}(\lambda)$ with its first-order Taylor expansion around $\lambda=4.5$, and thus evaluate λ^* from

$$\lambda^*\approx 4.5-\overline{c}(4.5)\left(\left.\frac{d\overline{c}}{d\lambda}\right|_{\lambda=4.5}\right)^{-1}. \tag{A7}$$

In order to compute $\overline{c}(4.5)$ we fit our data for $\overline{R}$ with ansatz (6), where we fix $\omega=0.8$. We have checked that the final result for λ^* has a very weak dependence on the value of ω used in the analysis. If we choose $\omega=0.75$, the results vary much less than the quoted error bar, indicating that the error on ω can be neglected.

As an example, the results for U_4 at $(Z_a/Z_p)_f=0.1944$ are given in Table X. We see that there is a slight drift toward larger values of $\overline{c}(4.5)$ as $L_{\min}$ is increased. The final result corresponds to $L_{\min}=16$ and $L_{\max}=96$. Systematic errors due to subleading corrections to scaling are estimated by comparing with the results obtained for $L_{\min}=8$ and $L_{\max}=48$. Assuming the errors on $\overline{c}(4.5)$ to decrease as $L^{-\omega_2+\omega}\approx L^{-0.8}$, we arrive at $\overline{c}(4.5)=0.0010(6)[19]$, where the systematic error is quoted in brackets.

In Table XI we give the analogous results for U_4 at $(\xi_{2\mathrm{nd}}/L)_f=0.5644$. Here we see a larger change of $\overline{c}(4.5)$ when $L_{\min}$ is varied. Also, χ^2/d.o.f. is larger for $L_{\min}<14$. Since corrections are larger than above, we take the final estimate from the fit with $L_{\min}=24$ and $L_{\max}=96$. We arrive at the estimate $\overline{c}(4.5)=0.002(2)[5]$. In a similar way we arrive at $\overline{c}(4.5)=0.007(5)[15]$ for U_6 at $(Z_a/Z_p)_f=0.1944$ and $\overline{c}(4.5)=0.003(4)[18]$ for U_6 at $(\xi_{2\mathrm{nd}}/L)_f=0.5644$.

Next, we compute $d\overline{c}/d\lambda$ at $\lambda=4.5$. To estimate the derivative of $\overline{c}(\lambda)$, we consider the finite differences

$$\left.\frac{d\overline{c}}{d\lambda}\right|_{\lambda=4.5}\approx[\overline{R}(L,5.0)-\overline{R}(L,4.0)]L^{\omega}. \tag{A8}$$

TABLE XII. Estimates of $[\overline{R}(L,5.0)-\overline{R}(L,4.0)]L^{\omega}$ with $\omega=0.8$.

L	U_4 at $(Z_a/Z_p)_f$	U_4 at $(\xi_{2\mathrm{nd}}/L)_f$	U_6 at $(Z_a/Z_p)_f$	U_6 at $(\xi_{2\mathrm{nd}}/L)_f$
6	−0.00957(17)	−0.01128(18)	−0.03141(53)	−0.03674(54)
8	−0.00951(21)	−0.01136(22)	−0.03111(67)	−0.03697(70)
10	−0.00973(25)	−0.01174(27)	−0.03164(80)	−0.03799(85)
12	−0.00972(28)	−0.01160(30)	−0.03150(88)	−0.03747(93)
14	−0.00983(33)	−0.01188(36)	−0.03201(105)	−0.03855(113)
16	−0.00972(37)	−0.01181(40)	−0.03183(115)	−0.03848(123)
18	−0.00972(47)	−0.01195(53)	−0.03177(148)	−0.03884(162)
20	−0.01022(57)	−0.01174(63)	−0.03392(179)	−0.03880(194)
22	−0.00947(68)	−0.01176(74)	−0.03074(213)	−0.03795(231)
24	−0.00962(79)	−0.01209(86)	−0.03128(249)	−0.03915(272)
28	−0.00962(124)	−0.01159(135)	−0.03208(388)	−0.03832(423)

TABLE XIII. Results for $[\overline{R}(L,5.0)-\overline{R}(L,\lambda)]/(5.0-\lambda)L^{\omega}$ with $\omega=0.8$ for $L\geqslant 12$. In the first row $\lambda=4.0$, and in the second row $\lambda=4.5$.

U_4 at $(Z_a/Z_p)_f$	U_4 at $(\xi_{2nd}/L)_f$	U_6 at $(Z_a/Z_p)_f$	U_6 at $(\xi_{2nd}/L)_f$
−0.00976(16)	−0.01177(17)	−0.03184(49)	−0.03823(53)
−0.00872(27)	−0.01035(29)	−0.02838(86)	−0.03356(92)

The results for our four choices of $\overline{R}$ are given in Table XII. We see that the results, as functions of L, are constant within error bars. This nicely confirms the exponent $\omega=0.8$.

The final result for the derivative is obtained by averaging the results for $L\geqslant 12$; see Table XIII. In order to estimate the discretization error, we additionally compute the derivative, using $\overline{R}(L,\lambda)$ for the pair $\lambda=5.0$ and 4.5. The difference with the above-reported result is small and in practice negligible, approximately 12% for U_4 at $(Z_a/Z_p)_f=0.1944$ and U_4 at $(\xi_{2nd}/L)_f=0.5644$, and approximately 14% for U_6 at $(Z_a/Z_p)_f=0.1944$ and U_6 at $(\xi_{2nd}/L)_f=0.5644$.

Inserting our numerical results for $\overline{c}(4.5)$ and $d\overline{c}/d\lambda$ into Eq. (A7), we obtain $\lambda^*=4.6(4)$, 4.7(8), 4.7(8), and 4.6(8) from U_4 at $(Z_a/Z_p)_f=0.1944$, U_4 at $(\xi_{2nd}/L)_f=0.5644$, U_6 at $(Z_a/Z_p)_f=0.1944$ and U_6 at $(\xi_{2nd}/L)_f=0.5644$, respectively. The errors take into account the uncertainty of $\overline{c}(4.5)$, $d\overline{c}/d\lambda|_{\lambda=4.5}$, and ω. As our final result we quote $\lambda^*=4.6(4)$ from U_4 at $(Z_a/Z_p)_f=0.1944$.

4. Critical exponents

We compute the critical exponents ν and η using standard FSS methods.

a. Exponent ν

The exponent ν is determined by fitting the data with Eq. (8). We study the derivative of all four quantities U_4, U_6, ξ_{2nd}/L, and Z_a/Z_p, and fix β_f by using either $(\xi_{2nd}/L)_f=0.5644$ or $(Z_a/Z_p)_f=0.1944$.

As typical examples, we give fit results for $\partial U_4/\partial\beta|_{\beta_f}$, $[\partial(Z_a/Z_p)/\partial\beta]|_{\beta_f}$, and $[\partial(\xi_{2nd}/L)/\partial\beta]|_{\beta_f}$ in Tables XIV, XV, and XVI, respectively. In all these three cases, we have fixed β_f by $(Z_a/Z_p)_f$. Fixing β_f by $(\xi_{2nd}/L)_f$ leads to similar results.

TABLE XIV. Estimates of ν from the fit of $\partial U_4/\partial\beta|_{\beta_f}$ with ansatz (8). β_f is fixed by $(Z_a/Z_p)_f=0.1944$.

L_{min}	L_{max}	χ^2/d.o.f.	ν
6	96	1.36	0.71215(16)
8	96	0.72	0.71174(20)
10	96	0.70	0.71179(26)
12	96	0.71	0.71160(34)
16	96	0.79	0.71137(49)
20	96	0.86	0.71167(66)

TABLE XV. Estimates of ν from the fit of $[\partial(Z_a/Z_p)/\partial\beta]|_{\beta_f}$ with the ansatz (8). β_f is fixed by $(Z_a/Z_p)_f=0.1944$.

L_{min}	L_{max}	χ^2/d.o.f.	ν
6	96	69.37	0.70660(6)
8	96	11.95	0.70837(8)
10	96	3.28	0.70918(11)
12	96	1.91	0.70969(15)
16	96	1.40	0.71009(22)
20	96	1.21	0.71054(30)
24	96	1.46	0.71044(46)
28	96	1.59	0.71071(58)

In the case of $\partial U_4/\partial\beta|_{\beta_f}$ we see that χ^2/d.o.f. is close to 1, even if all lattice sizes $L\geqslant 6$ are included in the fit. Also, the result for ν stays rather stable when L_{min} is increased.

On the other hand, for $[\partial(Z_a/Z_p)/\partial\beta]|_{\beta_f}$ and $[\partial(\xi_{2nd}/L)/\partial\beta]|_{\beta_f}$, χ^2/d.o.f. comes close to one only starting from $L_{min}\geqslant 16$. Also, the results for ν strongly change, when L_{min} is increased. It is interesting to notice that the estimate of ν is decreasing for $[\partial(\xi_{2nd}/L)/\partial\beta]|_{\beta_f}$ while it is increasing for $[\partial(Z_a/Z_p)/\partial\beta]|_{\beta_f}$ when L_{min} is increased. Assuming that this is already the asymptotic behavior, we can find lower and upper bounds for ν.

Taking into account the fit results for $L_{min}\geqslant 22$ we arrive at the final estimate $\nu=0.7113(10)$. Here the error bar includes both the statistical and the systematic error.

Finally, we try to determine the effect of leading corrections to scaling on our estimate of ν. For this purpose we fit our data up to $L_{max}=28$ at $\lambda=4.0$, 4.5, and 5.0 with ansatz (8). In Table XVII we give our results for the derivative of the Binder cumulant with respect to β at $(Z_a/Z_p)_f=0.1944$. In particular, for small L_{min}, we see a clear dependence of the result for ν on λ. For instance, for $L_{min}=8$ the difference between the result for $\lambda=4.0$ and $\lambda=5.0$ is 0.00176(46).

In Table XVIII we give the corresponding analysis for Z_a/Z_p at $(Z_a/Z_p)_f=0.1944$. In this case we see a much smaller dependence of the results for ν on λ. For $L_{min}=8$ the difference between the results for $\lambda=4.0$ and 5.0 is −0.00065(18). The behavior in the case of ξ_{2nd}/L (which is not shown here) is much the same: the dependence of the fit

TABLE XVI. Estimates of ν from the fit of $[\partial(\xi_{2nd}/L)/\partial\beta]|_{\beta_f}$ with ansatz (8). β_f is fixed by $(Z_a/Z_p)_f=0.1944$.

L_{min}	L_{max}	χ^2/d.o.f.	ν
6	96	68.10	0.71826(8)
8	96	18.76	0.71613(11)
10	96	7.72	0.71489(14)
12	96	4.35	0.71394(18)
16	96	1.32	0.71261(27)
20	96	1.43	0.71246(37)
24	96	1.27	0.71169(56)
28	96	1.39	0.71196(70)

TABLE XVII. Estimates of ν computed from the derivative of the Binder cumulant at β_f, where β_f is fixed by $(Z_a/Z_p)_f = 0.1944$.

$L_{\min}$	$L_{\max}$	χ^2/d.o.f.	ν
		$\lambda = 4.0$	
6	28	0.91	0.71301(24)
8	28	0.75	0.71269(33)
10	28	0.83	0.71296(44)
12	28	1.07	0.71275(64)
		$\lambda = 4.5$	
6	28	1.64	0.71226(17)
8	28	0.74	0.71181(23)
10	28	0.67	0.71193(32)
12	28	0.74	0.71170(46)
		$\lambda = 5.0$	
6	28	1.27	0.71153(23)
8	28	0.76	0.71093(32)
10	28	0.44	0.71034(43)
12	28	0.51	0.71014(60)

result for ν on λ is much smaller than for the Binder cumulant.

Taking into account the range the lattice sizes that are used to obtain the final result for ν, we arrive at a possible uncertainty of 0.0001 for ν from the derivative of Z_a/Z_p and of $\xi_{2\mathrm{nd}}/L$ due to the uncertainty in λ^*. The systematic error is clearly dominated by subleading corrections. Our final MC estimate of ν is

$$\nu = 0.7113(11). \tag{A9}$$

b. Exponent η

We determine the exponent η by using Eq. (10), and also a fit ansatz that includes a constant background term [Eq. (11)]. We fix β_f by setting either $(\xi_{2\mathrm{nd}}/L)_f = 0.5644$ or $(Z_a/Z_p)_f = 0.1944$.

TABLE XVIII. Estimates of ν computed from the derivative of Z_a/Z_p at β_f, where β_f is fixed by $(Z_a/Z_p)_f = 0.1944$.

$L_{\min}$	$L_{\max}$	χ^2/d.o.f.	ν
		$\lambda = 4.0$	
8	28	8.97	0.70766(13)
10	28	1.63	0.70871(18)
12	28	1.58	0.70902(27)
		$\lambda = 4.5$	
8	28	14.38	0.70804(9)
10	28	2.84	0.70890(13)
12	28	1.57	0.70941(19)
		$\lambda = 5.0$	
8	28	8.52	0.70831(13)
10	28	2.89	0.70916(18)
12	28	2.40	0.70965(25)

TABLE XIX. Estimates of η from fits of the magnetic susceptibility at $\lambda = 4.5$ with Eq. (10). β_f is fixed by $(Z_a/Z_p)_f = 0.1944$.

$L_{\min}$	$L_{\max}$	χ^2/d.o.f.	η
12	96	32.55	0.03557(5)
16	96	6.36	0.03641(7)
20	96	1.73	0.03682(9)
24	96	1.00	0.03710(13)
28	96	0.81	0.03725(16)
32	96	0.81	0.03740(24)

Fits for $\lambda = 4.5$ with the ansatz (10) are given in Tables XIX [β_f fixed by $(Z_a/Z_p)_f = 0.1944$] and XX [β_f fixed by $(\xi_{2\mathrm{nd}}/L)_f = 0.5644$]. In both cases, χ^2/d.o.f. becomes close to 1 starting from $L_{\min} = 24$. Moreover, in both cases the fit results for η are strongly increasing as $L_{\min}$ is increased. For $L_{\min} = 32$ we have a consistent result of $\eta = 0.0374(2)$.

Next, we checked the dependence of the result for η on λ. In Table XXI we give results for $\lambda = 4.0$, 4.5, and 5.0 for $L_{\min} = 16$ and $L_{\max} = 28$. We see a rather strong dependence on λ. The difference between the results for $\lambda = 4.0$ and 5.0 is 0.00080(25). Taking into account the range of lattice sizes used to obtain our final estimate, we arrive at an error of 0.0002 on η due to the error on λ^*.

Finally, we performed fits with ansatz (11). The results are summarized in Tables XXII and XXIII. We observe that a χ^2/d.o.f. close to 1 is already reached for $L_{\min} = 10$. Moreover, the result for η changes little with increasing $L_{\min}$. For $L_{\min} = 16$ the results obtained by fixing β_f by Z_a/Z_p and $\xi_{2\mathrm{nd}}/L$ agree. Therefore, as our final result we give $\eta = 0.0378(6)$. The error bar is such that it includes the result of the fits with ansatz (10).

APPENDIX B: ANALYSIS OF THE HIGH-TEMPERATURE EXPANSIONS

In this appendix we report a discussion of our HT analyses. It should allow the reader to understand how we determined our estimates and the reliability of the errors we report, which are to some extent subjective. More details on the methods we use are reported in Ref. 36.

1. Definitions and HT series

We computed the HT expansion of several quantities for the ϕ^4 lattice Hamiltonian [Eq. (1)] for generic values of λ

TABLE XX. Estimates of η from fits of the magnetic susceptibility at $\lambda = 4.5$ with Eq. (10). β_f is fixed by $(\xi_{2\mathrm{nd}}/L)_f = 0.5644$.

$L_{\min}$	$L_{\max}$	χ^2/d.o.f.	η
12	96	33.81	0.03592(4)
16	96	8.24	0.03656(5)
20	96	2.35	0.03695(7)
24	96	0.77	0.03725(10)
28	96	0.59	0.03735(12)
32	96	0.65	0.03742(18)

TABLE XXI. Estimates of η from fits of the magnetic susceptibility at $\lambda=4.0$, 4.5, and 5.0 with Eq. (10). β_f is fixed by $(Z_a/Z_p)_f=0.1944$.

λ	$L_{\min}$	$L_{\max}$	χ^2/d.o.f.	η
4.0	16	28	4.75	0.03610(18)
4.5	16	28	2.96	0.03562(13)
5.0	16	28	8.53	0.03530(18)

by using the linked-cluster expansion technique. A general introduction to this technique can be found in Refs. 110–112. We calculated the 20th-order HT expansion of the magnetic susceptibility and of the second moment of the two-point function,

$$\chi=\sum_x \langle\phi_\alpha(0)\phi_\alpha(x)\rangle, \quad m_2=\sum_x x^2\langle\phi_\alpha(0)\phi_\alpha(x)\rangle, \tag{B1}$$

and therefore, the second-moment correlation length $\xi^2=m_2/(6\chi)$. Moreover, we computed the HT expansion of the zero-momentum connected $2j$ point Green's functions χ_{2j}:

$$\chi_{2j}=\sum_{x_2,\ldots,x_{2j}} \langle\phi_{\alpha_1}(0)\phi_{\alpha_1}(x_2)\ldots\phi_{\alpha_j}(x_{2j-1})\phi_{\alpha_j}(x_{2j})\rangle_c \tag{B2}$$

($\chi=\chi_2$). More precisely, we computed χ_4 to 18th order, and χ_6, χ_8, and χ_{10} to 15th order. In Table XXIV we report the series for the ϕ^4 Hamiltonian with $\lambda=4.5$. We chose this value because it is very close to the best estimate of λ^*, and because for this value of λ we have a precise MC estimate of β_c, $\beta_c=0.6862385(20)$.

The HT series of the zero-momentum four-point coupling g_4 and of the coefficients r_{2j} that parametrize the small-magnetization expansion of the equation of state can be computed using their definitions in terms of χ_{2j} and ξ^2, i.e.,

$$g_4=-\frac{3N}{N+2}\frac{\chi_4}{\chi^2\xi^3}, \tag{B3}$$

and

$$r_6=10-\frac{5(N+2)}{3(N+4)}\frac{\chi_6\chi_2}{\chi_4^2},$$

TABLE XXII. Estimates of η from fits of the magnetic susceptibility at $\lambda=4.5$ with Eq. (11). β_f is fixed by $(Z_a/Z_p)_f=0.1944$.

$L_{\min}$	$L_{\max}$	χ^2/d.o.f.	η	b
8	96	2.18	0.03832(8)	−0.657(9)
10	96	1.22	0.03811(10)	−0.617(17)
12	96	0.72	0.03790(12)	−0.555(26)
16	96	0.66	0.03782(17)	−0.528(54)

TABLE XXIII. Estimates of η from fits of the magnetic susceptibility at $\lambda=4.5$ with Eq. (11). β_f is fixed by $(\xi_{2\text{nd}}/L)_f=0.5644$.

$L_{\min}$	$L_{\max}$	χ^2/d.o.f.	η	b
8	96	0.80	0.03756(6)	−0.379(6)
10	96	0.68	0.03765(7)	−0.396(11)
12	96	0.64	0.03772(9)	−0.416(20)
16	96	0.53	0.03780(13)	−0.454(39)

$$r_8=280-\frac{280(N+2)}{3(N+4)}\frac{\chi_6\chi_2}{\chi_4^2}+\frac{35(N+2)^2}{9(N+4)(N+6)}\frac{\chi_8\chi_2^2}{\chi_4^3}, \tag{B4}$$

$$r_{10}=15400-\frac{7700(N+2)}{(N+4)}\frac{\chi_6\chi_2}{\chi_4^2}+\frac{350(N+2)^2}{(N+4)^2}\frac{\chi_6^2\chi_2^2}{\chi_4^4}+\frac{1400(N+2)^2}{3(N+4)(N+6)}\frac{\chi_8\chi_2^2}{\chi_4^3}-\frac{35(N+2)^3}{3(N+4)(N+6)(N+8)}\frac{\chi_{10}\chi_2^3}{\chi_4^4}.$$

The formulas relevant for the Heisenberg universality class are obtained setting $N=3$.

2. Critical exponents

In order to estimate γ and ν, we analyzed the 20th-order HT expansion of the magnetic susceptibility and the 19th-order HT expansion of ξ^2/β. We analyzed the HT series by means of integral approximants[113] (IA's) of first, second, and third order (IA1's, IA2's and IA3's, respectively). Since the most precise results are obtained by using the MC estimates of β_c to bias the approximants, we shall only report the results of the biased analyses. We used the values of β_c obtained in Appendix A 2, i.e.,

$$\beta_c(\lambda=4.0)=0.6843895(35), \tag{B5}$$

$$\beta_c(\lambda=4.5)=0.6862385(20), \tag{B6}$$

$$\beta_c(\lambda=5.0)=0.6875638(37). \tag{B7}$$

We considered several sets of biased IA's, and for each of them we obtained estimates of the critical exponents. In the analysis we closely followed Ref. 36. Thus, in the following we shall heavily refer to it for notations and a more detailed description of the analyses.

Given an nth-order series $f(\beta)=\Sigma_{i=0}^n c_i\beta^i$, its kth-order integral approximant $[m_k/m_{k-1}/\cdots/m_0/l]$ IAk is a solution of the inhomogeneous kth-order linear differential equation

$$P_k(\beta)f^{(k)}(\beta)+P_{k-1}(\beta)f^{(k-1)}(\beta)+\cdots+P_1(\beta)f^{(1)}(\beta)+P_0(\beta)f(\beta)+R(\beta)=0, \tag{B8}$$

TABLE XXIV. Coefficients of the HT expansion of m_2, χ, χ_4, χ_6, χ_8, and χ_{10}, for the ϕ^4 Hamiltonian with $\lambda=4.5$.

i	m_2	χ_2	χ_4
0	0	0.9578480539072253262554 0	−0.1022068663188906646418 5
1	0.6116485962492392230634 0	1.8349457887477176691920 0	−0.7831891839960428631101 7
2	2.3434656703696799593135 2	3.0257052655569931495264 3	−3.4099330325119561443372 4
3	6.1263156380473488522406 4	4.9108427235701116769357 4	−11.454726114938742611165 4
4	13.741167801314822398470 8	7.7241368558362591140595 0	−32.862285760980707058893 8
5	28.180690773627160736412 6	12.069665111137451078269 8	−84.870377052266453606813 1
6	54.611011223115649597985 8	18.589874363960220343389 7	−203.04839194486132618348 0
7	101.60110632181055549022 6	28.512946968487537452485 2	−458.48707099190159646907 6
8	183.444896900967255684973	43.391041440043105625628 3	−989.113871576954399028213
9	323.515763329983708761073	65.845709721903394386288 0	−2056.80132192600410402482
10	560.008592676223985571196	99.431841560185688368691 5	−4148.88336851312159356144
11	954.596109677157386424652	149.842255361185424824490	−8158.09343927729005801740
12	1606.62254117132464855356	225.053071205898843291857	−15696.1032586702224741180
13	2674.82852285795544112124	337.491827618915172447234	−29637.6862646277928041257
14	4412.16935517377929559254	504.872666999718714410906	−55053.5845813513443015904
15	7219.36840082433737483629	754.353044416651842398902	−100803.117025457078176935
16	11729.5598928466629681760	1125.029163386959766441444	−182227.804691700019121686
17	18938.5632727811981324466	1676.217709341799616503 20	−325689.103869085626575337
18	30408.8505644977121915813	2493.832919871236960647 87	−576156.574987690512078391
19	48583.1353446096892196268	3707.296370737199011873 94	
20	77271.9486733817666941548	5504.791576690358240567 91	

i	χ_6	χ_8	χ_{10}
0	0.1685619778291961819080 19	−0.6160509091872289415266 3	3.9032386342583869894575 2
1	2.5642557604810363143772 82	−15.230009298713487730055 64	141.589060417753517915167
2	19.758339498833626636016 29	−178.37213716159503835137 49	2318.78554766886373709723
3	107.6153442827461300177955	−1404.03404775262637194221	24643.8854034121990204490
4	470.3177686849044939915090	−8533.18422765821528578124	196815.472836825966956507
5	1762.676494500452240334969	−43117.7286797414375624292	1278183.93414715336465143
6	5892.468315770018895075220	−189462.996356270457135473	7085909.43897471702725255
7	18026.10606034742588181350	−745826.772293316301527782	34639336.4985891651938076
8	51364.40898933529517266700	−2685696.43890603392620130	152792638.179196536855095
9	138079.9439575146969655288	−8982884.52144712077544905	618543549.844101982857471
10	353553.4243627006337358070	−28231531.3374765513159336	2328085189.97290506149579
11	868613.6815956677724696610	−84122578.3791382746491922	8229819042.53291083435060
12	2059460.213048375196521201	−239356596.354404154637789	27546203927.2418206714112
13	4734189.661963741454010320	−654084831.403386579980857	87876514492.4881461446469
14	10591072.53372872753915110	−1724768015.94141791734955	268647512699.595417711632
15	23130642.47447337362164738	−4405965912.50799258526090	790611696518.867100914318

where the functions $P_i(\beta)$ and $R(\beta)$ are polynomials of orders m_i and l, respectively, which are determined by the known nth-order small-β expansion of $f(\beta)$. We considered two types of biased IAk's:

(i) The first type of biased IAk's, which will be denoted by bIAk's, is obtained by setting

$$P_k(\beta)=(1-\beta/\beta_c)p_k(\beta), \tag{B9}$$

where $p_k(\beta)$ is a polynomial of order m_k-1.

(ii) Since on bipartite lattices $\beta=-\beta_c$ is also a singular point associated to the antiferromagnetic critical behavior,[114] we consider IAk's with

$$P_k(\beta)=(1-\beta^2/\beta_c^2)p_k(\beta), \tag{B10}$$

where $p_k(\beta)$ is a polynomial of order m_k-2. We shall denote them by $b_{\pm}$IAk's.

In our analyses we considered diagonal or quasidiagonal approximants, since they are expected to give the most accurate results. For each set of IAk's we calculated the average of the values corresponding to all nondefective IAk's.

TABLE XXV. Results for γ obtained from the analysis of the 20th-order HT series of χ.

λ	Approximants	r_a	γ
4.0	bIA1	(35−3)/48	1.39508(6)[32]
	bIA2	(77−7)/115	1.39503(16)[33]
4.5	bIA1	(36−3)/48	1.39585(4)[18]
	$b_{\pm}$IA1	(21−1)/48	1.39583(4)[18]
	bIA2	(93−11)/115	1.39580(10)[18]
	$b_{\pm}$IA2	(84−7)/100	1.39579(18)[18]
	bIA3	(56−6)/61	1.39582(5)[19]
5.0	bIA1	(34−3)/48	1.39652(6)[32]
	bIA2	(107−13)/115	1.39648(7)[34]

TABLE XXVI. Results for ν obtained from the analysis of the 19th-order series of ξ^2/β.

λ	Approximants	r_a	ν
4.0	bIA1	(37−6)/37	0.71061(1)[14]
	bIA2	(65−3)/70	0.71055(17)[14]
4.5	bIA1	(37−4)/37	0.71110(3)[8]
	$b_{\pm}$IA1	(31−3)/36	0.71111(2)[8]
	bIA2	(67−2)/70	0.71108(6)[7]
	$b_{\pm}$IA2	(54−3)/55	0.71114(3)[8]
	bIA3	(26−2)/34	0.71110(10)[10]
5.0	bIA1	(36−4)/37	0.71151(5)[15]
	bIA2	(67−5)/70	0.71154(6)[14]

Approximants are considered defective when they have singularities close to the real β axis near the critical point. We also discarded some nondefective IA's—we call them outliers—whose results are far from the average of the other approximants. All details can be found in Appendix B of Ref. 36.

In Tables XXV and XXVI we report the results for γ and ν, respectively, obtained by analyzing the series for $\lambda=4.0$, 4.5, and 5.0. There, we also quote the ''approximant ratio'' $r_a \equiv (g-f)/t$, where t is the total number of approximants in the given set, g is the number of nondefective approximants, and f is the number of outliers which are discarded using an algorithm described in Appendix B of Ref. 36; $g-f$ is the number of ''good'' approximants used in the analysis. Note that $g \gg f$, and $g-f$ is never too small. For each analysis, besides the corresponding estimate, we report two numbers. The number in parentheses, e_1, is basically the spread of the approximants for β_c fixed at its MC estimate. It is the standard deviation of the results obtained from all ''good'' IA's divided by the square root of r_a, i.e., $e_1=\sigma/\sqrt{r_a}$. The number in brackets, e_2, is related to the uncertainty on the value of β_c, and is estimated by varying β_c in the range $[\beta_c - \Delta\beta_c, \beta_c + \Delta\beta_c]$.

APPENDIX C: UNIVERSAL AMPLITUDE RATIOS FROM THE PARAMETRIC REPRESENTATION

In the following we report the expressions of the universal amplitude ratios in terms of the parametric representation [Eq. (43)] of the critical equation of state. The singular part of the free energy per unit volume can be written as

$$\mathcal{F}_{\rm sing} = h_0 m_0 R^{2-\alpha} g(\theta), \tag{C1}$$

where $g(\theta)$ is the solution of the first-order differential equation

$$(1-\theta^2) g'(\theta) + 2(2-\alpha)\theta g(\theta) = Y(\theta) h(\theta), \tag{C2}$$

that is regular at $\theta=1$. The function $Y(\theta)$ has been defined in Eq. (44). The longitudinal magnetic susceptibility can be written as

$$\chi_L^{-1} = \frac{h_0}{m_0} R^{\gamma} g_2(\theta), \quad g_2(\theta) = \frac{2\beta\delta\theta h(\theta) + (1-\theta^2) h'(\theta)}{Y(\theta)}. \tag{C3}$$

The function $g_2(\theta)$ must vanish at θ_0 in order to reproduce the predicted behavior at the coexistence curve $\chi_L \sim H^{-1/2}$, according to

$$g_2(\theta) \sim \theta_0 - \theta \quad \text{for} \quad \theta \to \theta_0. \tag{C4}$$

From Eq. (C3) we see that $g_2(\theta)$ satisfies this condition if $h(\theta) \sim (\theta_0-\theta)^2$ for $\theta \to \theta_0$.

From the equation of state one can derive universal amplitude ratios of zero-momentum quantities. We consider

$$U_0 \equiv A^+/A^- = (\theta_0^2-1)^{2-\alpha} \frac{g(0)}{g(\theta_0)}, \tag{C5}$$

$$R_\chi \equiv \frac{C^+ B^{\delta-1}}{B_c^\delta} = (\theta_0^2-1)^{-\gamma} [m(\theta_0)]^{\delta-1} [m(1)]^{-\delta} h(1), \tag{C6}$$

$$R_C \equiv \frac{\alpha A^+ C^+}{B^2} = -\alpha(1-\alpha)(2-\alpha)(\theta_0^2-1)^{2\beta} \times [m(\theta_0)]^{-2} g(0), \tag{C7}$$

$$R_4 \equiv -\frac{C_4^+ B^2}{(C^+)^3} = \rho^2 [m(\theta_0)]^2 (\theta_0^2-1)^{-2\beta}. \tag{C8}$$

Using Eqs. (45) and (47) one can easily derive the expressions of the various coefficients that characterize the asymptotic behavior of the scaling functions $f(x)$ and $F(z)$, such as c_f, f_i^0 for $f(x)$ and F_i^∞, r_{2j} for $F(z)$. Concerning the ratios involving amplitudes along the crossover line, one finds

$$P_m \equiv \frac{T_p^\beta B}{B_c} = x_{\rm max}^\beta f(x_{\rm max})^{-1/\delta}, \tag{C9}$$

$$P_c \equiv -\frac{T_p^{2\beta\delta} C^+}{C_4} = F(z_{\rm max})^{-2}, \tag{C10}$$

$$R_p \equiv \frac{C^+}{C_p} = F'(z_{\max}). \tag{C11}$$

Here $x_{\max}$ and $z_{\max}$ are the values of the scaling variables x and z computed at $\theta_{\max}$, where $\theta_{\max}$ is the solution of the equation

$$\beta \delta F[z(\theta)]F''[z(\theta)] - \gamma F'[z(\theta)]^2 = 0. \tag{C12}$$

*Email address: Massimo.Campostrini@df.unipi.it
†Email address: Martin.Hasenbusch@desy.de
‡Email address: Andrea.Pelissetto@roma1.infn.it
§Email address: Paolo.Rossi@df.unipi.it
‖Email address: Ettore.Vicari@df.unipi.it

[1] The isotropic Heisenberg model is a simplified model, and neglects several interactions that are present in real materials. Among them, we should mention the cubic anisotropies due to the lattice structure and the dipolar interactions. Even if, in the renormalization-group language, these effects are relevant perturbations of the Heisenberg fixed point (see Refs. 115–118), the critical exponents are so close to those of the Heisenberg universality class that the difference is experimentally very difficult to observe, see, e.g., Refs. 119, 118, 120, and 56, and references therein.

[2] M. Shaham, J. Barak, U. El-Hanany, and W.W. Warren, Jr., Phys. Rev. B **22**, 5400 (1980).

[3] M.A. Kobeissi, Phys. Rev. B **24**, 2380 (1981).

[4] M. Seeger, S.N. Kaul, H. Kronmüller, and R. Reisser, Phys. Rev. B **51**, 12 585 (1995).

[5] R. Reisser, R.K. Kremer, and A. Simon, Phys. Rev. B **52**, 3546 (1995).

[6] J.H. Zhao, H.P. Kunkel, X.Z. Zhou, G. Williams, and M.A. Subramanian, Phys. Rev. Lett. **83**, 219 (1999).

[7] S.G. Barsov, A.L. Getalov, V.P. Koptev, S.A. Kotov, S.M. Mikirtychyants, G.V. Shcherbatov, A.A. Arsenov, and Ya.M. Mukovskii, Physica B **289-290**, 81 (2000).

[8] J.H. Zhao, T. Song, H.P. Kunkel, X.Z. Zhou, R.M. Roshko, and G. Williams, J. Phys.: Condens. Matter **12**, 6903 (2000).

[9] C.S. Arnold and D.P. Pappas, Phys. Rev. Lett. **85**, 5202 (2000).

[10] J. Mira, J. Rivas, A. Butera, L.B. Steren, J.M. García-Beneytez, and M. Vázquez, J. Appl. Phys. **87**, 5911 (2000).

[11] C. Bührer, M. Bechmann, M. Fähnle, U. Grünewald, and K. Maier, J. Magn. Magn. Mater. **212**, 211 (2000).

[12] T. Brückel, D. Hupfeld, J. Strempfer, W. Caliebe, K. Mettenberger, A. Stunault, N. Bernhoeft, and G.J. McIntyre, Eur. Phys. J. B **19**, 475 (2001).

[13] F.Y. Yang, C.L. Chien, X.W. Li, G. Xiao, and A. Gupta, Phys. Rev. B **63**, 092403 (2001).

[14] C.S. Hong, W.S. Kim, and N.H. Hur, Phys. Rev. B **63**, 092504 (2001).

[15] For some dopings and some divalent cation A, a first-order transition has been observed. Moreover, in systems in which the transition appears to be of second order, mean-field critical exponents have been measured. For instance, for $La_{1-x}Sr_xMnO_3$, a mean-field value for β was observed in Refs. 121–123, while an estimate compatible with the Heisenberg value was found in Refs. 124–127. For $x=1/3$ there also exists (Ref. 94) an estimate of the exponent α, $\alpha=-0.14\pm0.10$, in agreement with the Heisenberg value.

[16] In order to observe the correct exponents, it is essential to consider corrections to scaling in the analysis of the experimental data (Ref. 24). All results reported in Table II, except those of Ref. 21, have been obtained by assuming scaling corrections of the form $(1+a|t|^{\Delta_1}+b|t|^{\Delta_2})$, with $\Delta_1=0.11$ and $\Delta_2=0.55$. Two observations are in order here. First, the results of the present paper provide a precise estimate of Δ_1, $\Delta_1=0.1336(15)$. Second, the renormalization group also predicts corrections of order $|t|^{2\Delta_1}$, $|t|^{3\Delta_1}$, etc. which are more relevant than the term $|t|^{\Delta_2}$, and should therefore be taken into account in the analysis of the data.

[17] S.N. Kaul and M. Sambasiva Rao, J. Phys.: Condens. Matter **6**, 7403 (1994).

[18] M. Sambasiva Rao and S.N. Kaul, J. Magn. Magn. Mater. **140-144**, 1567 (1995).

[19] M. Sambasiva Rao and S.N. Kaul, J. Magn. Magn. Mater. **147**, 149 (1995).

[20] P.D. Babu and S.N. Kaul, J. Phys.: Condens. Matter **9**, 7189 (1997).

[21] M.R. Said, Y.A. Hamam, I. Abu-Alyarayesh, and S. Mahmood, J. Magn. Magn. Mater. **195**, 679 (1999).

[22] A. Perumal, V. Srinivas, V.V. Rao, and R.A. Dunlap, Physica B **292**, 164 (2000).

[23] A. Perumal, V. Srinivas, K.S. Kim, S.C. Yu, V.V. Rao, and R.A. Dunlap, J. Magn. Magn. Mater. **233**, 280 (2001).

[24] S.N. Kaul, J. Magn. Magn. Mater. **53**, 5 (1985).

[25] A. Pelissetto and E. Vicari, Phys. Rev. B **62**, 6393 (2000).

[26] S.N. Kaul, Phys. Rev. B **38**, 9178 (1988).

[27] O. Källbäck, S.G. Humble, and G. Malmström, Phys. Rev. B **24**, 5214 (1981).

[28] B. Stroka, J. Wosnitza, E. Scheer, H. von Löhneysen, W. Park, and K. Fischer, Z. Phys. B: Condens. Matter **89**, 39 (1992).

[29] M. Marinelli, F. Mercuri, S. Foglietta, and D.P. Belanger, Phys. Rev. B **54**, 4087 (1996).

[30] H.G. Ballesteros, L.A. Fernández, V. Martín-Mayor, and A. Muñoz Sudupe, Phys. Lett. B **441**, 330 (1998).

[31] H.G. Ballesteros, L.A. Fernández, V. Martín-Mayor, A. Muñoz Sudupe, G. Parisi, and J.J. Ruiz-Lorenzo, J. Phys. A **32**, 1 (1999).

[32] M. Hasenbusch, K. Pinn, and S. Vinti, Phys. Rev. B **59**, 11 471 (1999).

[33] M. Hasenbusch, J. Phys. A **32**, 4851 (1999).

[34] M. Hasenbusch and T. Török, J. Phys. A **32**, 6361 (1999).

[35] M. Hasenbusch, Habilitationsschrift, Humboldt-Universität zu Berlin, 1999; Int. J. Mod. Phys. C **12**, 911 (2001).

[36] M. Campostrini, M. Hasenbusch, A. Pelissetto, P. Rossi, and E. Vicari, Phys. Rev. B **63**, 214503 (2001).

[37] M. Hasenbusch, J. Phys. A **34**, 8221 (2001).

[38] M. Campostrini, A. Pelissetto, P. Rossi, and E. Vicari, Phys. Rev. E **60**, 3526 (1999).

[39] M. Campostrini, A. Pelissetto, P. Rossi, and E. Vicari, Phys. Rev. B **61**, 5905 (2000).

[40] P. Butera and M. Comi, Phys. Rev. B **56**, 8212 (1997).

[41] A.A. Caparica, A. Bunker, and D.P. Landau, Phys. Rev. B **62**, 9458 (2000).

[42] H.G. Ballesteros, L.A. Fernández, V. Martín-Mayor, and A.

Muñoz Sudupe, Phys. Lett. B **387**, 125 (1996).
[43] C. Holm and W. Janke, Phys. Rev. B **48**, 936 (1993); Phys. Lett. A **173**, 8 (1993); J. Appl. Phys. **73**, 5488 (1993).
[44] P. Peczak, A.M. Ferrenberg, and D.P. Landau, Phys. Rev. B **43**, 6087 (1991).
[45] J. Adler, C. Holm, and W. Janke, Physica A **201**, 581 (1993).
[46] F. Jasch and H. Kleinert, J. Math. Phys. **42**, 52 (2001).
[47] R. Guida and J. Zinn-Justin, J. Phys. A **31**, 8103 (1998).
[48] D. B. Murray and B. G. Nickel, Guelph University report, 1991 (unpublished).
[49] J.C. Le Guillou and J. Zinn-Justin, Phys. Rev. Lett. **39**, 95 (1977); Phys. Rev. B **21**, 3976 (1980).
[50] V.I. Yukalov and S. Gluzman, Phys. Rev. E **58**, 1359 (1998).
[51] H. Kleinert, Phys. Lett. A **264**, 357 (2000).
[52] K.E. Newman and E.K. Riedel, Phys. Rev. B **30**, 6615 (1984).
[53] O. Bohr, B.-J. Schaefer, and J. Wambach, Int. J. Mod. Phys. A **16**, 3823 (2001).
[54] G.v. Gersdorff and C. Wetterich, Phys. Rev. B **64**, 054513 (2001).
[55] J. Berges, N. Tetradis, and C. Wetterich, Phys. Rev. Lett. **77**, 873 (1996).
[56] A. Pelissetto and E. Vicari, cond-mat/0012164 (unpublished).
[57] Recently, a model with competing superexchange and double-exchange interactions was studied (Ref. 128). A preliminary analysis for the paramagnetic-ferromagnetic transition gives $\nu = 0.720(2)$ and $\gamma = 1.438(8)$. While ν is reasonable agreement with the Heisenberg value, γ is significantly higher, so that the identification of this transition as a Heisenberg one is in doubt.
[58] G.A. Baker, Jr., B.G. Nickel, M.S. Green, and D.I. Meiron, Phys. Rev. Lett. **36**, 1351 (1977); G.A. Baker, Jr., B.G. Nickel, and D.I. Meiron, Phys. Rev. B **17**, 1365 (1978).
[59] K.G. Chetyrkin, S.G. Gorishny, S.A. Larin, and F.V. Tkachov, Phys. Lett. B **132**, 351 (1983).
[60] H. Kleinert, J. Neu, V. Schulte-Frohlinde, K.G. Chetyrkin, and S.A. Larin, Phys. Lett. B **272**, 39 (1991); **319**, 545(E) (1993).
[61] S. Hikami and E. Brézin, J. Phys. A **11**, 1141 (1978).
[62] S. Hikami, Nucl. Phys. B **215**, 555 (1983).
[63] W. Bernreuther and F.J. Wegner, Phys. Rev. Lett. **57**, 1383 (1986).
[64] J. Berges, N. Tetradis, and C. Wetterich, hep-ph/0005122 (unpublished).
[65] P. Butera and M. Comi, Phys. Rev. B **60**, 6749 (1999).
[66] I.M. Mryglod, I.P. Omelyan, and R. Folk, Phys. Rev. Lett. **86**, 3156 (2001).
[67] In the so-called critical-point renormalization method (see Ref. 129, and references therein), given two series $D(x)$ and $E(x)$ that are singular at the same point x_0, $D(x)=\Sigma_i d_i x^i \sim (x_0 - x)^{-\delta}$ and $E(x)=\Sigma_i e_i x^i \sim (x_0-x)^{-\epsilon}$, one constructs a series $F(x)=\Sigma_i (d_i/e_i)x^i$. The function $F(x)$ is singular at $x=1$, and for $x \to 1$ behaves as $F(x) \sim (1-x)^{-\phi}$, where $\phi = 1+\delta-\epsilon$. Therefore, the difference $\delta-\epsilon$ can be obtained by analyzing the expansion of $F(x)$ by means of biased approximants with a singularity at $x_c=1$.
[68] E. Brézin and D.J. Wallace, Phys. Rev. B **7**, 1967 (1973).
[69] E. Brézin and J. Zinn-Justin, Phys. Rev. B **14**, 3110 (1976).
[70] D.J. Wallace and R.P.K. Zia, Phys. Rev. B **12**, 5340 (1975).
[71] L. Schäfer and H. Horner, Z. Phys. B: Condens. Matter **29**, 251 (1978).
[72] I.D. Lawrie, J. Phys. A **14**, 2489 (1981).
[73] A. Pelissetto and E. Vicari, Nucl. Phys. B **540**, 639 (1999).
[74] M. Barmatz, P.C. Hohenberg, and A. Kornblit, Phys. Rev. B **12**, 1947 (1975).
[75] E. Brézin, D.J. Wallace, and K.G. Wilson, Phys. Rev. Lett. **29**, 591 (1972); Phys. Rev. B **7**, 232 (1973).
[76] R. Guida and J. Zinn-Justin, Nucl. Phys. B **489**, 626 (1997).
[77] M. Caselle, M. Hasenbusch, A. Pelissetto, and E. Vicari, J. Phys. A **34**, 2923 (2001).
[78] M. Campostrini, A. Pelissetto, P. Rossi, and E. Vicari, Phys. Rev. B **62**, 5843 (2000).
[79] J. Zinn-Justin, *Quantum Field Theory and Critical Phenomena*, 3rd ed. (Clarendon Press, Oxford, 1996).
[80] P. Butera and M. Comi, Phys. Rev. B **58**, 11 552 (1998).
[81] A. Pelissetto and E. Vicari, Nucl. Phys. B **575**, 579 (2000).
[82] A. Pelissetto and E. Vicari, Nucl. Phys. B **519**, 626 (1998); Nucl. Phys. B (Proc. Suppl.) **73**, 775 (1999).
[83] T. Reisz, Phys. Lett. B **360**, 77 (1995).
[84] A.I. Sokolov, E.V. Orlov, V.A. Ul'kov, and S.S. Kashtanov, Phys. Rev. E **60**, 1344 (1999).
[85] A. Pelissetto and E. Vicari, Nucl. Phys. B **522**, 605 (1998).
[86] N. Tetradis and C. Wetterich, Nucl. Phys. B **422**, 541 (1994).
[87] P. Schofield, Phys. Rev. Lett. **22**, 606 (1969).
[88] P. Schofield, J.D. Lister, and J.T. Ho, Phys. Rev. Lett. **23**, 1098 (1969).
[89] B.D. Josephson, J. Phys. C **2**, 1113 (1969).
[90] In the HT phase $t>0$, $Mt^{-\beta} = g(Ht^{-\beta\delta})$ where $g(\tau)$ is analytic in the complex τ plane except possibly for two branch cuts on the imaginary axis, for $|\mathrm{Im}\,\tau| > \tau_0$ (Yang-Lee theorem). Thus the convergence radius is at most $|z| < |g(i\tau_0)|/k$, where k is the normalization of z.
[91] S.A. Larin, M. Mönnigmann, M. Strösser, and V. Dohm, Phys. Rev. B **58**, 3394 (1998).
[92] C. Bervillier, Phys. Rev. B **34**, 8141 (1986).
[93] H. Kleinert and B. Van den Bossche, Phys. Rev. E **63**, 056113 (2001).
[94] C.A. Ramos, H.R. Salva, R.D. Sanchez, M. Tovar, F. Rivadulla, J. Mira, J. Rivas, A.M. Lopez-Quintela, L. Hueso, M. Saint-Paul, P. Lejay, and Y. Tokura, J. Magn. Magn. Mater. **226-230**, 582 (2001).
[95] R. Abe and M. Masutani, Prog. Theor. Phys. **59**, 672 (1978).
[96] M. Stroesser, S.A. Larin, and V. Dohm, Nucl. Phys. B **540**, 654 (1999).
[97] A. Aharony and P.C. Hohenberg, Phys. Rev. B **13**, 3081 (1976).
[98] C. Bagnuls and C. Bervillier, Phys. Rev. B **32**, 7209 (1985).
[99] C. Bervillier, Phys. Rev. B **14**, 4964 (1976).
[100] C. Bervillier and C. Godrèche, Phys. Rev. B **21**, 5427 (1980).
[101] The amplitudes B, B_c, and C^+ were determined in several experiments—see, e.g., Ref. 20—and thus an estimate of the ratio R_χ is possible. However, these amplitudes have large systematic uncertainties, and we can only obtain a rough estimate, $0.6 \lesssim R_\chi \lesssim 2$.
[102] V. Privman, P. C. Hohenberg, and A. Aharony, in *Phase Transitions and Critical Phenomena*, edited by C. Domb and J.L. Lebowitz (Academic Press, New York, 1991), Vol. 14.
[103] J.S. Kouvel and D.S. Rodbell, Phys. Rev. Lett. **18**, 215 (1967).
[104] S.F. Fischer, S.N. Kaul, and H. Kronmüller, J. Magn. Magn. Mater. **226-230**, 540 (2001).
[105] A. Arrott and J.E. Noakes, Phys. Rev. Lett. **19**, 786 (1967).
[106] We have evaluated $(u_{\mathrm{expt}})_{\max}$ (the position of the maximum) from Fig. 4 of Ref. 6: $(u_{\mathrm{expt}})_{\max} \approx 0.0005$. The variable u defined in Sec. IV D is related to u_{expt} by $u = u_{\mathrm{expt}}/(u_{\mathrm{expt}})_{\max}$. Note that the $(u_{\mathrm{expt}})_{\max}$ can also be derived from a knowledge of the non-

universal constants B, B_c, and C^+, and using the results of Sec. IV D. Indeed,

$$(u_{\mathrm{expt}})_{\max}=\left(\frac{B_c}{B}\right)^{1/\beta} w_{\max}=\left(\frac{C^+}{B_c}\right)^{1/\gamma} w_{\max}R_\chi^{-1/\gamma}$$

$$=\left(\frac{C^+}{B}\right)^{1/(\beta\delta)} w_{\max}R_\chi^{-1/(\beta\delta)}.$$

Numerically, using the estimates reported in Sec. IV D, we have $w_{\max}=1.55(6)$, $w_{\max}R_\chi^{-1/\gamma}=1.28(7)$, and $w_{\max}R_\chi^{-1/(\beta\delta)}=1.33(7)$.

[107] K. Binder, Z. Phys. B: Condens. Matter **43**, 119 (1981); Phys. Rev. Lett. **47**, 693 (1981).

[108] M. Hasenbusch, Physica A **197**, 423 (1993).

[109] A.P. Gottlob and M. Hasenbusch, J. Stat. Phys. **77**, 919 (1994).

[110] M. Wortis, in *Phase Transitions and Critical Phenomena*, edited by C. Domb and M.S. Green (Academic Press, London, 1974), Vol. 3.

[111] M. Lüscher and P. Weisz, Nucl. Phys. B **300**, 325 (1988).

[112] M. Campostrini, J. Stat. Phys. **103**, 369 (2001).

[113] For a review see, e.g., A.J. Guttmann, in *Phase Transitions and Critical Phenomena*, edited by C. Domb and J. Lebowitz (Academic, New York, 1989), Vol. 13.

[114] M.E. Fisher, Philos. Mag. **7**, 1731 (1962).

[115] M.E. Fisher, Rev. Mod. Phys. **46**, 597 (1974).

[116] A. Aharony, in *Phase Transitions and Critical Phenomena*, edited by C. Domb and J. Lebowitz (Academic Press, New York, 1976), Vol. 6, p. 357.

[117] A. Aharony and M.E. Fisher, Phys. Rev. B **8**, 3323 (1973).

[118] J.M. Carmona, A. Pelissetto, and E. Vicari, Phys. Rev. B **61**, 15 136 (2000).

[119] A.D. Bruce and A. Aharony, Phys. Rev. B **10**, 2078 (1974).

[120] S. Srinath, S.N. Kaul, and M.-K. Sostarich, Phys. Rev. B **62**, 11 649 (2000).

[121] S.E. Lofland, V. Ray, P.H. Kim, S.M. Bhagat, M.A. Manheimer, and S.D. Tyagi, Phys. Rev. B **55**, 2749 (1997).

[122] C.V. Mohan, M. Seeger, H. Kronmüller, P. Murugaraj, and J. Maier, J. Magn. Magn. Mater. **83**, 348 (1998).

[123] A. Schwartz, M. Scheffler, and S.M. Anlage, Phys. Rev. B **61**, R870 (2000).

[124] M.C. Martin, G. Shirane, Y. Endoh, K. Hirota, Y. Moritomo, and Y. Tokura, Phys. Rev. B **53**, 14 285 (1996).

[125] R.H. Heffner, L.P. Le, M.F. Hundley, J.J. Neumeier, G.M. Luke, K. Kojima, B. Nachumi, Y.J. Uemura, D.E. MacLaughlin, and S.-W. Cheong, Phys. Rev. Lett. **77**, 1869 (1996).

[126] S.E. Lofland, S.M. Bhagat, K. Ghosh, R.L. Greene, S.G. Karabashev, D.A. Shulyatev, A.A. Arsenov, and Y. Mukovskii, Phys. Rev. B **56**, 13 705 (1997).

[127] K. Ghosh, C.J. Lobb, R.L. Greene, S.G. Karabashev, D.A. Shulyatev, A.A. Arsenov, and Y. Mukovskii, Phys. Rev. Lett. **81**, 4740 (1998).

[128] S.-H. Tsai and D.P. Landau, J. Magn. Magn. Mater. **226-230**, 650 (2001).

[129] D.L. Hunter and G.A. Baker, Jr., Phys. Rev. B **7**, 3346 (1973); **7**, 3377 (1973); Phys. Rev. B **19**, 3808 (1979); M.E. Fisher and H. Au-Yang, J. Phys. A **12**, 1677 (1979); **13**, 1517(E) (1980); A.J. Guttmann and G.S. Joyce, *ibid.* **5**, L81 (1972); J.J. Rehr, A.J. Guttmann, and G.S. Joyce, *ibid.* **13**, 1587 (1980).